

**ÇOKLU CİSİMLER DİNAMİĞİ YAKLAŞIMIYLA
MAKARALI RULMAN MODELİNİN GELİŞTİRİLMESİ:
RULMAN TİTREŞİM İLETİM YOLU ANALİZİ**

**DEVELOPMENT OF A ROLLER BEARING MODEL FOR
MULTIBODY SIMULATIONS:
BEARING VIBRATION TRANSFER PATH ANALYSIS**

UMUT TEKTÜRK

ASSOC. PROF. DR. SELAHATTİN ÇAĞLAR BAŞLAMIŞLI

Supervisor

Submitted to

Graduate School of Science and Engineering of Hacettepe University

as a Partial Fulfillment to the Requirements

for the Award of the Degree of Master

in Mechanical Engineering

2020

This work titled “**Development of a Roller Bearing Model for Multibody Simulations: Bearing Vibration Transfer Path Analysis**” by **UMUT TEKTÜRK** has been approved as a thesis for the Degree of **Master of Science in Mechanical Engineering** by the Examining Committee Members mentioned below

Asst. Prof. Dr. Selçuk HİMMETOĞLU

Head

Assoc. Prof. Dr. Selahattin Çağlar BAŞLAMIŞLI

Supervisor

Assoc. Prof. Dr. Mesut DÜZGÜN

Member

Assoc. Prof. Dr. Mehmet Bülent Özer

Member

Asst. Prof. Dr. Bilsay SÜMER

Member

This thesis has been approved as a thesis for the Degree of **Master of Science in Mechanical Engineering** by board of Directors of the Institute of Graduate School of Science and Engineering on / /.....

Prof. Dr. Salih Bülent ALTEN

Director of Institute of

Graduate School of Science and Engineering

To my mother...

ETHICS

In this thesis study, prepared in accordance with the spelling rules of Institute of Graduate School of Science and Engineering of Hacettepe University,

I declare that

- all the information and documents have been obtained in the base of the academic rules
- all audio-visual and written information and results have been presented according to the rules of scientific ethics
- in case of using other works, related studies have been cited in accordance with the scientific standards
- all cited studies have been fully referenced
- I did not do any distortion in the data set
- and any part of this thesis has not been presented as another thesis study at this or any other university.

07/12/ 2020

UMUT TEKTÜRK

YAYINLANMA FİKRİ MÜLKİYET HAKKLARI BEYANI

Enstitü tarafından onaylanan lisansüstü tezimin/raporumun tamamını veya herhangi bir kısmını, basılı (kağıt) ve elektronik formatta arşivleme ve aşağıda verilen koşullarla kullanıma açma iznini Hacettepe üniversitesine verdiğimi bildiririm. Bu izinle Üniversiteye verilen kullanım hakları dışındaki tüm fikri mülkiyet haklarım bende kalacak, tezimin tamamının ya da bir bölümünün gelecekteki çalışmalarda (makale, kitap, lisans ve patent vb.) kullanım hakları bana ait olacaktır.

Tezin kendi orijinal çalışmam olduğunu, başkalarının haklarını ihlal etmediğimi ve tezimin tek yetkili sahibi olduğumu beyan ve taahhüt ederim. Tezimde yer alan telif hakkı bulunan ve sahiplerinden yazılı izin alınarak kullanması zorunlu metinlerin yazılı izin alarak kullandığımı ve istenildiğinde suretlerini Üniversiteye teslim etmeyi taahhüt ederim.

Yükseköğretim Kurulu tarafından yayınlanan “*Lisansüstü Tezlerin Elektronik Ortamda Toplanması, Düzenlenmesi ve Erişime Açılmasına İlişkin Yönerge*” kapsamında tezim aşağıda belirtilen koşullar haricince YÖK Ulusal Tez Merkezi / H. Ü. Kütüphaneleri Açık Erişim Sisteminde erişime açılır.

- Enstitü / Fakülte yönetim kurulu kararı ile tezimin erişime açılması mezuniyet tarihimden itibaren 2 yıl ertelenmiştir.
- Enstitü / Fakülte yönetim kurulu gerekçeli kararı ile tezimin erişime açılması mezuniyet tarihimden itibaren ay ertelenmiştir.
- Tezim ile ilgili gizlilik kararı verilmiştir.

..... / /

UMUT TEKTÜRK

ABSTRACT

DEVELOPMENT OF A ROLLER BEARING MODEL FOR MULTIBODY SIMULATIONS: BEARING VIBRATION TRANSFER PATH ANALYSIS

Umut TEKTÜRK

Master of Science, Department of Mechanical Engineering

Supervisor: Assoc. Prof. Dr. Selahattin Çağlar BAŞLAMİŞLİ

December 2020, 68 pages

Mechanical systems are major sources of sound radiations and vibrations, even in their good operating conditions. The vibro-acoustic transfer functions of mechanical systems are crucial in Noise Vibration Harshness (NVH) analysis. Rotating machines are among common applications in mechanical engineering. Every mechanical component in rotating machines affect the total vibration transfer path. For this reason, for an accurate NVH modelling of the system, the detailed modelling of each component is required.

With the advancements in commercial multibody simulation software and computational capacity of the modern computers, it is possible to model and simulate complex multibody systems. Rolling bearings are considered as the key elements in motion and vibration transmission. They are utilized to carry shaft and transmit the motion. Therefore, rolling bearings need to be modelled accurately by considering their varying dynamic characteristics.

A number of studies have proposed and investigated various bearing dynamic models to estimate their dynamical behavior. Although available models have widely being used in

industry and academia, their accuracy in estimation of bearing vibrations and vibration transfer path is still doubtful. In this regard, modelling and implementation of the rolling bearing contact mechanism plays major role in bearing vibration transfer path function. Rolling bearing contacts are usually considered as Hertz contact in the literature. In contrast, the recent investigations show the importance of the Elastohydrodynamic (EHD) contacts in dynamic modelling of mechanical parts. The EHD contacts can be simulated and analyzed using Reynolds and Computational Fluid Dynamics (CFD).

Within the objectives of the current study, three rolling bearing dynamic models based on three various contact models using, Hertz, Reynolds, and CFD are developed. For this purpose, bearing contacts are considered as Kelvin-Voigt spring-dampers, and extended to a total rolling bearing model in a Multibody Simulation (MBS) environment. Then, their dynamic properties and transfer paths are investigated and compared numerically in the time and frequency domain. The numerical results illustrate and highlight the differences and limitations of the above mentioned bearing contact modelling methods in the context of the total bearing model.

Key Words: cylindrical rolling bearing, multibody dynamics, multibody simulation, modal analysis, noise-vibration-harshness.

ÖZET

ÇOKLU CİSİMLER DİNAMİĞİ YAKLAŞIMIYLA MAKARALI RULMAN MODELİNİN GELİŞTİRİLMESİ: RULMAN TİTREŞİM İLETİM YOLU ANALİZİ

Umut TEKTÜRK

Yüksek Lisans, Makina Mühendisliği Bölümü

Tez Danışmanı: Doç. Dr. Selahattin Çağlar BAŞLAMİŞLİ

Aralık 2020, 68 sayfa

Mekanik sistemler, temel ses yayılımı ve titreşim kaynaklarıdır. Gürültü, titreşim ve sertlik (NVH) analizlerinde mekanik sistemlerin titreşim-akustik transfer fonksiyonları etkilidir. Dönen makinalar, makina mühendisliğinde yaygın uygulamalar arasındadır. Bu makinalardaki her mekanik bileşen, toplam titreşim aktarım yoluna etki eder. Bu nedenle, mekanik bir sistemin hassas ve gerçeğe yakın bir NVH modelinin çıkarılması için her bir sistem bileşeninin ayrıntılı olarak modellenmesi gereklidir.

Ticari çoklu cisimler simülasyonu yazılımlarındaki gelişmeler ile modern bilgisayarların hesaplama kapasitelerindeki ilerlemeler, karmaşık çoklu cisim sistemlerini modellemek ve simülasyonlarını gerçekleştirmeye olanak tanımaktadır. Rulmanlar, dönen milleri taşımak ve hareketi iletmek için kullanılmalarının yanında hareket ve titreşim aktarımında

temel unsurlar olarak kabul edilmektedirler. Bu nedenle rulmanların deęişen dinamik özellikleri dikkate alınarak doğru bir şekilde modellenmesi gereklidir.

Yapılan çalışmalarda, rulman dinamik davranışlarını öngörebilmek için çeşitli rulman dinamik modelleri önerilmiştir. Mevcut modeller endüstride ve akademide yaygın olarak kullanılmasına rağmen, yatak titreşimleri ve titreşim aktarım yolunun tahminindeki doğrulukları hala tartışılmaktadır. Bu bağlamda, makaralı rulman temas mekanizmasının modellenmesi ve uygulanması, rulman titreşim aktarım yolu fonksiyonunda büyük rol oynamaktadır. Rulman temasları, literatürde genellikle Hertz temas ilişkisi olarak kabul edilir. Bununla birlikte, son araştırmalar, mekanik sistem elemanlarının dinamik modellemesinde Elastohidrodinamik (EHD) temasların önemini göstermektedir. EHD temasları Reynolds ve Hesaplamalı Akışkanlar Dinamiği (CFD) yöntemleri kullanılarak modellenebilir ve analiz edilebilir.

Bu çalışma kapsamında, Hertz, Reynolds ve CFD yöntemleri kullanılarak, farklı temas modellerine dayanan rulman dinamik modelleri geliştirilmiştir. Bu amaçla, rulman temasları Kelvin-Voigt yay-sönümleyici olarak kabul edilmiş ve Çoklu Cisimler Simülasyonu (MBS) ortamında tam rulman modeline genişletilmiştir. Daha sonra dinamik özellikleri ve titreşim iletim yolları incelenmiş ve sonuçlar zaman ve frekans alanında sayısal olarak karşılaştırılmıştır. Sayısal sonuçlar, tam yatak modeli bağlamında yukarıda bahsedilen rulman teması modelleme yöntemlerinin farklılıklarını ve sınırlarını göstermiş ve vurgulamıştır.

Anahtar Kelimeler: silindirik makaralı rulman, çoklu cisimler dinamiği, çoklu cisimler simülasyonu, modal analiz, titreşim-gürültü- sertlik.

ACKNOWLEDGMENTS

This study was carried out with the cooperation of Hacettepe University and RWTH Aachen University. A large number of people were involved in the creation of this work. I would like to express my appreciation to all of these people in the following.

I would like to express my appreciation to my supervisor Assoc. Prof. Dr. S. Çağlar BAŞLAMIŞLI for his support and guidance throughout my thesis study.

During this study, I was an exchange student at RWTH Aachen University. I would like to thank Mr. Assist. Prof. Selçuk Himmetoglu, who is Hacettepe University Mechanical Engineering Department Erasmus Coordinator, Ahmet Efe Belli who is department secretary and all members of European Union Office for their support in this process.

This work was conducted at Machine Elements and System Engineering Institute of RWTH Aachen University. I am appreciated all members of the institute, especially Mr. Dr.-Ing., Univ. Prof. Georg Jacobs, Mr. Dr.-Ing. Joerg Berroth and Mr. Reza Golafshan, M.Sc. who gave me the opportunity to do this work.

As an advisor and a mentor, I am really grateful to Mr. Reza Golafshan, M.Sc. for his limitless support, patience and friendship. He is more than an advisor for me.

I would like to thank Mr. Stefan Wischmann, M.Sc. for his help about bearing modelling and simulation processes. Whenever I need help, he gave me his hand.

I would also like to thank members of Laboratory for Machine Tools and Production Engineering of RWTH Aachen University, especially Mr. Tobias Motscke, M.Sc., who carried out the tests within the scope of the thesis.

I am thankful to my friends Ayhan Arda Araz, Koray Beyaz, Mirsahand Miralizadeh Jalalat, Bahman Kheradmandi and all my friends for their precious friendship and support.

Special thanks goes to my love and my best friend, Hilal Topçu, for her endless support, patience, and unconditional love.

I am grateful to my parents, Rabia and Memduh Tektürk for their support and encouragement during my life. I was lost my mother during my thesis study due to cancer. I want to devote this work to my mother.

TABLE OF CONTENT

ABSTRACT.....	i
ÖZET	iii
ACKNOWLEDGMENTS	v
TABLE OF CONTENT.....	vii
LIST OF FIGURES	ix
LIST OF TABLES.....	xii
SYMBOLS AND ABBREVIATIONS.....	xiii
1. INTRODUCTION	1
1.1. Problem Description	1
1.2. Objectives	2
1.3. Method.....	3
1.4. Used Tools	5
2. FUNDAMENTALS.....	6
2.1. Cylindrical Roller Bearing.....	6
2.1.1. Types of Cylindrical Roller Bearings	6
2.1.2. Bearing Geometry.....	7
2.1.3. Load Distribution on Bearing	7
2.1.4. Roller Profile.....	8
2.1.5. Bearing Kinematics.....	9
2.1.6. Bearing Contact Force Calculation.....	10
2.1.6.1 Contact Stiffness for Line Contact.....	10
2.1.6.2 Contact Damping	11
2.2. Multibody Simulation	14
2.2.1. Flexible Body Application in MBS	15
2.2.2. Bearing Modelling in MBS.....	17
2.3. Modal Analysis	18
2.3.1. Numerical Approach.....	18
2.3.2. Linear System Analysis	19

2.3.3. Experimental Approach.....	20
2.4. Case Study on Bearing Contact Dynamics	22
3. DYNAMIC MODELLING OF CYLINDRICAL ROLLER BEARING	28
3.1. Model Development in Simpack.....	29
3.2. Modelling of Bearing Kinematics	30
3.2.1. Position and Orientation of Rings	30
3.2.2. Position and Orientation of Rolling Elements.....	32
3.3. Bearing Contact Stiffness Calculation	34
3.3.1. Applied Load Bearing	34
3.3.2. Contact Detection	35
3.4. EHD Bearing Model.....	35
3.5. Validation of Developed Bearing Models.....	37
4. INVESTIGATIONS ON EHD BASED MODELS	43
4.1. Study on Bearing Testrig: On one single operating point.....	43
4.1.1. Modelling and Simulations	43
4.1.2. Experiment and Discussion	46
4.2. Bearing Simulations Using Continues EHD Characteristic Model	48
5. GEARBOX SYSTEM SIMULATIONS.....	52
6. GEARBOX EXPERIMENTS	57
6.1. Testrig.....	57
6.2. Results and Discussions	58
7. CONCLUSION	63
7.1. Summary	63
8. REFERENCES.....	65
CURRICULUM VITAE	68

LIST OF FIGURES

Figure 1.1. Scheme of modelling approach using in this study	5
Figure 2.1. Cylindrical roller bearing geometry, adapted from [3]	7
Figure 2.2. Load distribution on bearing under radial load	8
Figure 2.3. Schematic of roller profile.....	8
Figure 2.4. Pressure distribution of rollers with applied loads a) straight b) logarithmic c) crowned profiles from [1]	9
Figure 2.5. Velocities and speeds of cylindrical roller bearing, adapted from [3]	9
Figure 2.6. EHL in line contact from [5]	12
Figure 2.7. Damping and Stiffness in EHL from [5]	12
Figure 2.8. Pressure assumption in Reynolds Equation.....	13
Figure 2.9. A multibody system from [21]	15
Figure 2.10. A Flexible multibody system (steam engine) from [23]	16
Figure 2.11. Aliasing and Shannon's Theorem, adapted from [30]	21
Figure 2.12. N1014 bearing model in Simpack	23
Figure 2.13. The work flow of the CFD simulations.....	24
Figure 2.14. Rigid shaft bearing system	25
Figure 2.15. Shaft and bearing interaction in 2D representation	26
Figure 2.16. LSA Comparison of discrete data models w.r.t. Excitation E1 and Sensor S1	26
Figure 2.17. Zoomed version of Figure 2.16	27
Figure 3.1: Forces and moments inside a bearing	28
Figure 3.2. The developed model flow chart for contact force calculations	29
Figure 3.3. System flow chart for User-Force	30
Figure 3.4. Coordinates of inner ring displayed in user routine, adapted from [27]	32
Figure 3.5. Rolling elements movements in circumferential direction, adapted from [27]	33
Figure 3.6. Possible roller positions for a radially loaded bearing, adapted from [27] ..	33
Figure 3.7. Roller geometry with slices	34
Figure 3.8. Radial Penetration, from [27].....	35
Figure 3.9. EHD Contact Modelling Approach.....	36
Figure 3.10. Rigid shaft-bearing system in Simpack.....	37

Figure 3.11. Generated Force in bearings in y direction w.r.t. Excitation: E1-E2, Response: S1	39
Figure 3.12. LSA comparison of bearing models w.r.t. Excitation: E1-E2, Response: S1	40
Figure 3.13. LSA of CFD model for various velocities w.r.t. Excitation: E1-E2, Response: S1	40
Figure 3.14. LSA of CFD model for various forces w.r.t. Excitation: E1-E2, Response: S1	41
Figure 4.1. Shaft assembly model in Abaqus	44
Figure 4.2. Housing assembly model in Abaqus	44
Figure 4.3. Flexible model in Simpack	45
Figure 4.4. LSA results of Testrig w.r.t. excitation: E1 and sensor: S1	45
Figure 4.5. Bearing testrig	46
Figure 4.6. Comparison of Simulation and Experimental results	47
Figure 4.7. eMBS shaft-bearing-housing model in Simpack	48
Figure 4.8. Generated total radial force in bearings w.r.t. Excitation: E1, Response: S1	49
Figure 4.9. LSA comparison of eMBS bearing models w.r.t. Excitation: E1, Response: S1	50
Figure 4.10. Mode Shapes of Hertzian based eMBS models	50
Figure 4.11. CFD model for various rotational velocities w.r.t. Excitation: E1, Response: S1	51
Figure 4.12. CFD model for applied various forces w.r.t. Excitation: E1, Response: S1	51
Figure 5.1. Flexible gearbox model in Simpack	52
Figure 5.2. Campbell Diagram of eMBS gearbox with subroutine CFD bearing model	53
Figure 5.3. Detailed views of Figure 5.2	54
Figure 5.4. LSA results of gearbox	54
Figure 5.5. Percentage parameter changing in bearing contact	55
Figure 5.6. Campbell Diagram of eMBS gearbox with subroutine Hertzian based bearing model	56
Figure 6.1. Gearbox testrig	57
Figure 6.2. Campbell Diagram of gearbox testrig w.r.t. sensor 1	58

Figure 6.3. Sections from Figure 6.2	59
Figure 6.4.LSA results of gearbox testrig for different velocities w.r.t. sensor 1	60
Figure 6.5. Comparison of simulation and testrig results for section B w.r.t. sensor 1 ...	61
Figure 6.6. Sum level experiment results for various models	61

LIST OF TABLES

Table 2.1. Damping calculation coefficients.....	14
Table 2.2. Properties of N1014 Cylindrical Roller Bearing.....	22
Table 2.3. Obtained CFD Models Operational Conditions.....	24
Table 2.4. Bearing Contact Parameters for Various Contact Models	25
Table 3.1. Bearing Properties and Operational Conditions of CFD Simulations	37
Table 3.2. Properties of NU308 type bearing.....	38
Table 4.1. Operating conditions and dynamic paramters of CFD based discrete model.	43
Table 6.1. Details of gearbox testrig	58

SYMBOLS AND ABBREVIATIONS

Symbols

d_i	inner ring outer diameter
d_o	outer ring inner diameter
d_m	pitch diameter
D	roller diameter
D_{EHD}	elastohydrodynamic damping value
D_i	inner ring inner diameter
D_o	outer ring outer diameter
E	modulus of elasticity
F	force
f_e	viscous damping coefficient
h	film thickness
$h(t)$	excitation vector
$[H(w)]$	frequency response matrix
k	stiffness
L	roller length
$M(t)$	inertia matrix
n	angular velocity
P_d	diameteral clearance
$P(t)$	velocity dependent forces
$Q(t)$	position dependent forces
Q	load
s	slip ratio
$x(t)$	position vector

V	translational velocity
ν	poisson ratio
Λ	film parameter
μ	traction coefficient
ρ_0	contact pressure
ρ	density
α	contact angle
δ	deflection
$[\lambda^2]$	eigenvalue matrix
$[\Phi]$	eigenvector
θ	tilting angle

Abbreviations

AST	Alternative Slicing Technique
BC	Boundary Condition
BFRF	Body Fixed Reference Frame
CFD	Computational Fluid Dynamics
DOF	Degree of Freedom
EHD	Elastohydrodynamic
EHL	Elastohydrodynamic Lubrication
EOM	Equation of Motion
FBI	Flexible Body Input
FEM	Finite Element Method
FE88	Force Element 88
FRF	Frequency Response Function
LSA	Linear System Analysis

MBS	Multibody Simulation
MSE	Institut für Maschinenelemente und Systementwicklung
NVH	Noise, Vibration, Harshness
RFP	Rational Fraction Polynomial
UF	User Force
WZL	Werkzeugmaschinenlabor WZL der RWTH Aachen

1. INTRODUCTION

Mechanical systems are major sources of noise and vibrations. The vibro-acoustic transfer functions of the mechanical systems are important in dynamic analyses. Rotating machines are commonly used in various mechanical systems. Every mechanical component in the rotating machines affect the total vibration transfer path. For this reason, modelling of each part of the mechanical system is crucial, in order to build an accurate Noise Vibration Harshness (NVH) model.

With the advancements in commercial multibody simulation software and computational capacity of the modern computers, it is possible to simulate complex dynamics of multibody systems. Rolling bearings are considered as the key elements in motion transmission. Bearings are utilized to carry the shaft and to transmit the motion. However, due to the varying dynamic characteristics, bearings produce noise and vibration while performing their duty.

A number of studies have proposed various bearing dynamic models, in order to estimate their dynamic behaviour. Although these models are widely used in industry and widely accepted by the academic community, their accuracy in estimation of bearing vibration path is still doubtful. Hertzian contact is mainly used as rolling bearing contacts in literature. However, recent investigations show the importance of the Elastohydrodynamic (EHD) contacts in dynamic modelling of mechanical components. The EHD contacts can be determined using Reynolds and Computational Fluid Dynamics (CFD) approaches.

1.1. Problem Description

In dynamic system analysis, developing an accurate and a reliable model is a crucial step in estimating the system behaviour. The dynamic model can then be employed for NVH optimization purposes. The detailed models of the parts ensure realistic and reliable results. Nevertheless, as the model complexity increases, it becomes less practical due to the increasing simulation time and effort. Thus, there is a trade-off between model accuracy and applicability.

An accurate bearing model needs to include components of bearing and their detailed interactions. A typical rolling bearing model should contain rings, cage, rollers, rib,

lubrication effects and their corresponding interactions. There are many approaches in the literature to determine the component interactions of the bearing models [1]. Especially, Hertzian and EHD contact calculations are used to obtain the roller-raceway contact forces. Although Hertzian contact model is used in many studies, it considers only solid-solid contact interactions. Hertzian model calculations include geometric and material parameters, and it neglects the lubrication effect on roller-raceway contact dynamics. Hence, Hertzian contact model does not provide accurate results. EHD contact model include both solid and fluid interactions, and it considers lubricant effect on roller-raceway contact. Therefore EHD contact model ensures more realistic results than Hertzian model.

The Hertzian or EHD contact models affect the bearings dynamic behavior, and models may yield different results under various operation conditions (i.e. load, temperature, velocity, lubricant viscosity etc.). The selection of operation conditions can have an impact on the accuracy of the results and computation time. The parameters, which change with respect to operational conditions such as load and velocity, can be named as operational parameters, and operational parameters may affect the bearing dynamic behaviour.

The detailed model simulations need more computation effort, and the modelling structure has an important role on the computation effort. Creating a simple, comprehensible and modular system can reduce the simulation time. Furthermore, the model should be extendable, especially with the new technologies.

1.2. Objectives

The main objectives of the current study are listed below:

- Developing an open-source, extendable and modular cylindrical roller bearing model as a basis to investigate the bearing dynamic behavior.
- Investigating the reliability of Hertz and EHD based bearing contact models in predicting the bearing dynamics at the total system level.

One of the main objectives of this study is creating a new cylindrical roller bearing model. A simple and extendable model does not only provide easy integration of different contact models, but it also provides a base for future studies. A modular and clearly coded model

reduces the simulation time, computational effort and allows the model to be modified and extended as needed.

Another goal of this work is to compare the available rolling bearing contact models and investigate the accuracy and reliability of these models. For this purpose, contact forces, which are already obtained using Hertzian and EHD approaches, are extended to the total bearing model in a Multibody Simulation (MBS) environment. The Hertzian contact relation is used to calculate solid-solid contact forces, and EHD approach is used to calculate lubricated contact forces. The force calculations focus on normal forces, which include spring and damper forces. The contact force relations, which are about solid-solid and solid-oil stiffness and damping, concentrate the inner ring-roller and outer ring-roller contact relation. Calculated contact forces are integrated in the bearing model. In this regard, rigid and flexible shaft-bearing models are used to verify the bearing model. The developed total bearing model is then applied to a test gearbox model. In order to study the effect of the bearing model, the vibration transfer path of the system is examined in time and frequency domain.

The technical objectives of this study can be expressed as follows.

- Creating a new bearing model
- Implementing Hertz and EHD based bearing models in MBS environment
- Investigating the impact of the operational parameters on Hertzian and EHD based bearing models
- Analyzing the effect of different bearing modelling approaches on the entire system dynamic behaviour.

1.3. Method

The current study aims to model a test roller bearing in MBS environment. For this purpose, bearing contact force calculation model is provided by MSE Tribology Department [2], and the model is used within the context of this study. Bearing contacts are considered as Kelvin-Voigt spring-dampers, and extended to a total rolling bearing model. The contact of roller bearing components and the lubrication fluid between the components behave as a parallel spring-damper system. Damping forces occur due to the velocity differences between the components and spring forces occur due to the displacement differences between the components. Spring stiffness is defined as the force

required to cause a unit deflection on the spring, and the relation between damping force and velocity is named as damping constant. Hertzian and EHD contact properties are used for stiffness and damping calculations. The line contact equation is used to obtain Hertzian contact characteristics for cylindrical roller-raceway contacts. In addition to the Hertzian contacts, Reynolds equations and CFD methods can also be employed to conduct EHD contact calculations.

Simpack is MBS software, which provides opportunities for users to create their own force calculations via subroutines. Subroutines are used for building subprograms in FORTRAN programming languages. With the help of subroutines, a program can be divided into small programs, thus the program can have a modular structure. The subroutine that will be developed will then be integrated with the MBS tool to perform time integration of the dynamic model.

The obtained roller bearing model will be analyzed in the MBS environment. At first, rigid body simulations are conducted for shaft-bearing-housing system, and then, the model is integrated into a flexible shaft-bearing-housing system. Finally, a flexible gearbox model is examined using new bearing model. The systems are operated with various operational conditions and the effects of the obtained model on the vibrations and noise in the whole systems will be measured. The vibro-acoustic behaviour of a mechanical system can mainly be determined by the systems natural frequencies and mode shapes. Time domain simulations are also used to investigate the dynamic behaviours of mechanical systems. The systems are analysed using Linear System Analysis (LSA) and eigenvalue analysis in frequency domain. LSA estimates the excited behaviour of the linearized system. With this approach, the response of the vibration transfer path of the systems on bearing examined in frequency domain. While eigenvalues represent the natural frequencies of a system, eigenvectors represents the system mode shapes. Time integration, which is available in MBS software, is used to obtain the total behaviour of the multibody system in time domain analysis. These methods are repeated for various contact models (Hertzian and EHD), and the models are compared with each other.

A test gearbox and test shaft-bearing-housing systems are used to validate simulation results. In order to perform the flexible multibody simulations, Finite Element (FE) models are created based on test benches. On the other hand, experimental modal analyses

are performed to extract mode shapes and frequency response of the test systems. Campbell diagrams of the gearbox simulation model and test gearbox are considered to examine entire system dynamic behaviour. Campbell diagram is 3 dimensional plot, which shows the relationships between rotational speed, frequency and amplitude of the vibration signal.

The modelling, simulation and validation processes of the thesis are shown in Figure 1.1.

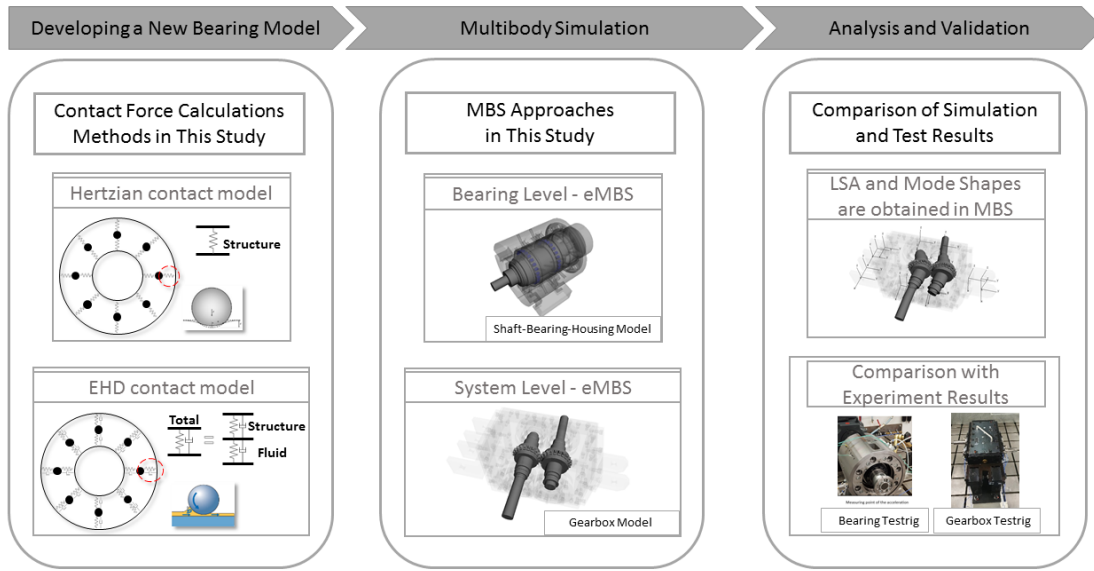


Figure 1.1. Scheme of modelling approach using in this study

1.4. Used Tools

Various software, programming languages and tools are required to conduct the analysis and to complete the modelling process.

MBS Software Simpack is employed to develop and apply a new cylindrical roller bearing model. Simpack provides facilities to extend the Simpack Element Library with their own modelling elements. The model creation process is conducted with FORTRAN programming language, and the model is transferred Simpack via user routine as a User-defined Force Element, in short user force. The simulations are performed, and results are evaluated with Modal analysis, LSA and time integration via Simpack as well.

It is crucial that the system components are modelled as flexible bodies in order to analyse the system vibration transfer path. For this reason, the flexible bodies such as shafts, housings, gears and bearing rings are constituted with the Abaqus software. The model reduction techniques are applied for transferring the system to Simpack.

2. FUNDAMENTALS

This study aims to investigate the effects of bearing contact models on the dynamics of mechanical systems. The bearing contact force calculations are related to bearing type, geometry, kinematic, lubrication, stiffness and damping. N1014 and NU308 types of cylindrical roller bearings are selected for the study. The simulations are conducted in MBS environment and results are analyzed in time and frequency domains.

In this section, the fundamentals of the previous studies on the bearing modelling is explained in some details. At first, the details of the cylindrical roller bearings with their geometrical, kinematic and dynamic properties are examined. Then, some basic aspects of multibody simulation as well as modal analysis is presented.

2.1. Cylindrical Roller Bearing

Roller bearings are required to overcome the speed difference between a rotating shaft and its surrounding structure. The bearing components are rollers, outer ring, inner ring, cage and rib. The bearings are grooved which allows both rings to roll. These grooves are called raceways. Roller bearings are used with a lubricant to reduce the vibration and friction. The surrounding structure of the roller bearing is called housing which provides significant static support to the shafts. In practice, rolling bearings are one of the excitation sources in rotating machines.

Cylindrical roller bearings have high radial and low axial load carrying capacities. They are convenient for high speed applications due to their low friction-torque characteristics [3].

2.1.1. Types of Cylindrical Roller Bearings

Cylindrical roller bearings are classified with respect to their ribs on their rings. NU and N type bearings can move freely on the ribless rings in axial direction. They are known as floating bearings. While NJ type bearings just support one directional axial load, NUP types generally provide reversing axial forces. Moreover, the internal design of the bearings can be changed to reach higher load carrying capacities [4].

Cylindrical roller bearings also classified with respect to their cage structures. Inner ring guidance, outer ring guidance and roller guidance cages are three types of cylindrical bearings [5]. For outer and inner ring guided cages, the cage is integrated with outer and inner ring. While outer ring has a shoulder for outer ring guided cage, inner ring has a

shoulder for inner ring guided cage. These shoulders provide axial support for rollers. For roller guided cage, the cage is placed between the rings with equal distance.

2.1.2. Bearing Geometry

The kinematics and dynamics of the bearings are related with the bearing geometry. Therefore, the geometrical properties of the bearing have an important role in the bearing simulations. Geometrical properties of cylindrical roller bearings are shown in Figure 2.1. The elements of the bearing are placed on the center positions. The terms in Figure 2.1, d_i , d_o , D_i , D_o , D , L , d_m , P_d are inner ring outer diameter (raceway), outer ring inner diameter (raceway), inner ring inner diameter, outer ring outer diameter, roller diameter, roller length, pitch diameter and diametral clearance, respectively.

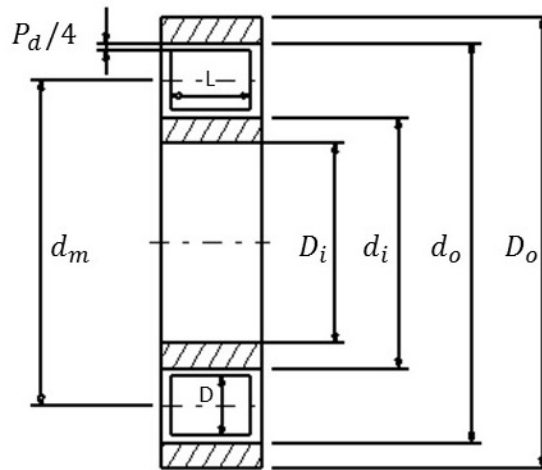


Figure 2.1. Cylindrical roller bearing geometry, adapted from [3]

Bearing pitch diameter is the mean of the inner and outer raceway diameter [3].

$$d_m = (d_i + d_o)/2 \quad (1)$$

Most bearings have diametral clearance, which provides free rotation between roller and raceway [3].

$$P_d = d_m - d_i - 2D \quad (2)$$

2.1.3. Load Distribution on Bearing

When a bearing is operating under radial loads, a load distribution is formed as shown in Figure 2.2. In the load zone, contact forces are much larger than the unloaded regions. The load distribution of a bearing is determined with the geometries of the bearing parts. Number of rolling elements and radial clearance have major roles, while the load zone arises. Moreover, preloads have an influence of the load distribution as well.

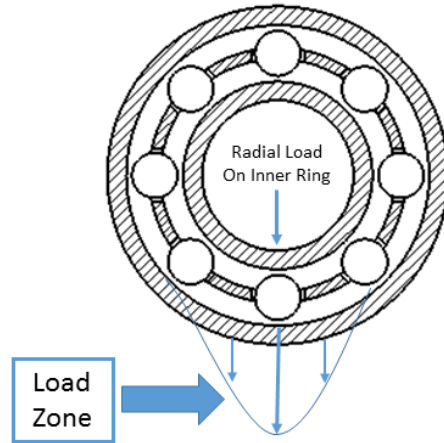


Figure 2.2. Load distribution on bearing under radial load

2.1.4. Roller Profile

Rollers are crowned along their length direction to avoid high pressure concentration on their end faces. Roller geometries are determined with the relation between roller length and roller diameter according to DIN 281-4 [6].

$$P(x_i) = 0.00035D \ln \left[\frac{1}{1 - \left(\frac{2|x_i|}{L} \right)^2} \right] \quad \text{for } L < 2.5D \quad (3)$$

$$P(x_i) = 0 \quad \text{for } |x_i| \leq \frac{L-2.5D}{2} \quad (4)$$

$$P(x_i) = 0.0005D \ln \left[\frac{1}{1 - \left(\frac{2|x_i| - (L-2.5D)}{L} \right)^2} \right] \quad \text{for } |x_i| > \frac{L-2.5D}{2} \quad (5)$$

Figure 2.3 shows the roller profile, which includes cylindrical and logarithmic sections.

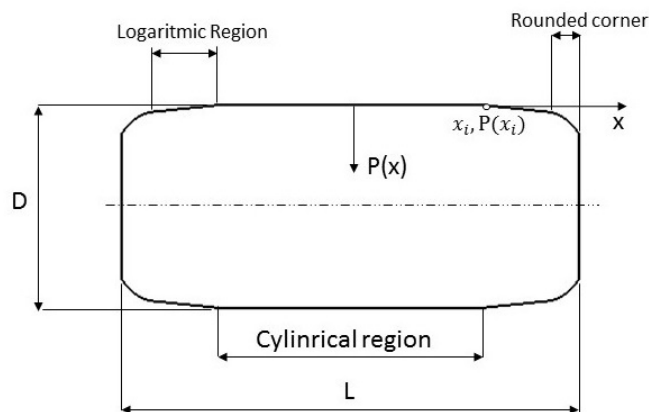


Figure 2.3. Schematic of roller profile

Figure 2.4 shows the pressure distribution of rollers with different profiles.

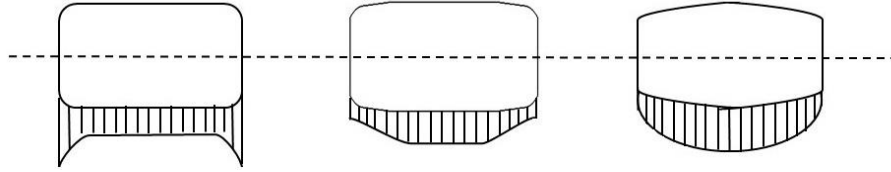


Figure 2.4. Pressure distribution of rollers with applied loads a) straight b) logarithmic c) crowned profiles from [1]

2.1.5. Bearing Kinematics

When bearings rotate at low speed, their behaviours are supposed to be kinematic. In such cases, rollers could roll without slip on raceways, and friction effects can be ignored. This phenomenon is known as kinematic action [3]. Figure 2.5 illustrates the kinematic analysis of the bearing.

While both inner and outer rings can rotate, α is the contact angle between roller and raceway. According to the Figure 2.5;

$$V_i = \frac{1}{2} w_i d_m (1 - \gamma) \quad (6)$$

$$V_o = \frac{1}{2} w_o d_m (1 + \gamma) \quad (7)$$

$$V_m = \frac{1}{2} (v_i + v_o) \quad (8)$$

$$n_m = \frac{1}{2} [n_i (1 - \gamma) + n_o (1 + \gamma)] \quad (9)$$

$$n_R = \frac{d_m}{2D} (1 - \gamma)(1 + \gamma)(n_o - n_i) \quad (10)$$

where, $\gamma = \frac{D}{d_m} \cos \alpha$.

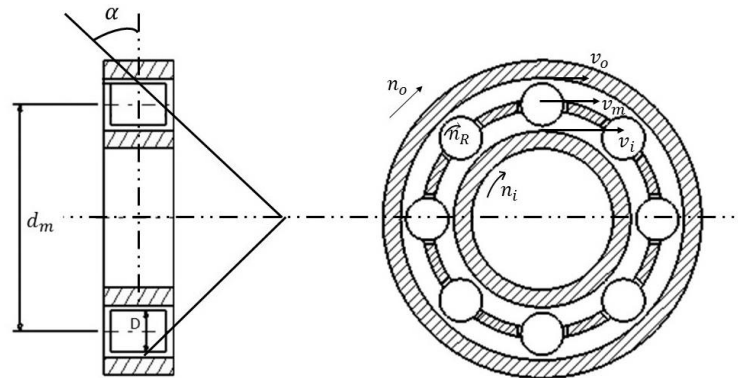


Figure 2.5. Velocities and speeds of cylindrical roller bearing, adapted from [3]

If outer ring remains stationary (i.e. $n_o = 0$), then

$$n_m = \frac{1}{2} n_i (1 - \gamma) \quad (11)$$

$$n_R = \frac{d_m n_i}{2D} (1 - \gamma)^2 \quad (12)$$

When bearing rotates due to contact frictions, lubricant churning moment and the other effects; rollers and cage have slippages [4]. The roller slip is determined by:

$$s_R = \frac{n_R - n_{RA}}{n_R} \times 100\% \quad (13)$$

where, s_R and n_{RA} are roller slip and actual time varying velocity of roller, respectively.

The cage slip is determined as:

$$s_m = \frac{n_m - n_{ma}}{n_m} \times 100\% \quad (14)$$

where, s_m is cage slip and n_{ma} is actual time varying velocity of cage.

2.1.6. Bearing Contact Force Calculation

There are five main contact forces in the bearings, namely inner raceway-roller, outer raceway-roller, roller-end surface, cage pocket- roller and roller-rib contact forces. The current study is mainly focused on contact normal forces between rollers and raceways. Bearing contact normal forces can be modelled by considering corresponding contact stiffness and damping forces.

2.1.6.1 Contact Stiffness for Line Contact

Heinrich Hertz has proposed and explained the interaction between load and deflection in point contact of elastic solids. In line contact case such as cylindrically shapes bodies, his approach was used to evaluate maximum contact pressure and the semi width of the contact [7].

$$b = \sqrt{\frac{8(1-\nu^2)Q}{\pi E \Sigma \rho L}} \quad (15)$$

$$\rho_0 = \frac{2}{\pi} \frac{Q}{bL} \quad (16)$$

$$\Sigma \rho = \frac{1}{R_1} \pm \frac{1}{R_2} \quad (17)$$

where, b is semi-width of contact, ν is poisson ratio, Q is normal load, E is modulus of elasticity, ρ is reduced radius, L is contact length, ρ_0 is maximum contact angle and $R_{1,2}$ is radius of contact bodies.

The convex-convex contact indicates the positive sign, while convex-concave contact indicates the negative sign. However, there is no explicit expressions in these equations.

Many Researchers studied the relation between load and deflection in the literature. Lundberg stated that the cylinders should have a specific profile to prevent stress concentrations at the end surfaces [8]. Kowalsky examined the deformation of a two-sided loaded cylinder with an elliptically distributed pressure [9]. Dinnik reached the parabolic pressure distribution over the width of the contact [10]. Palmgren referred that the roller diameter didn't affect the deflection from his experiments [11]. Kunert determined that there was no uniformly distributed pressure for line contact, and he considered the improved roller profile [12]. Houpert created curve fits for inner and outer raceway-roller contacts according to Tripp [13].

In order to obtain a more basic and less time-consuming load-deflection relationships, Teutsch and Sauer utilized previous works. They improved classical slicing technique and suggested a new method which is called an "Alternative Slicing Technique" (AST) [14]. The classical slicing technique divides rolling elements into the slices and each slice is considered independently. According to AST, however, the deformation of each slice is calculated by superimposing of individual weighted loads acting on all slices. In other words, slices are considered to be dependent on their deformation. As a result, AST also takes roller kinematics such as tilting and skewing into account.

2.1.6.2 Contact Damping

Damping is an important part of the bearing dynamics [15]. There are many different damping sources in rolling bearings. They can be summarized as [16],

- 1) Lubricant film damping on roller-raceway contacts,
- 2) Material hysteresis damping sources from deformation of the rolling bodies,
- 3) Damping originated from outer ring-housing or inner ring- shaft interaction.

The solid components of the bearing have very low damping with respect to oil damping. Therefore, oil damping is supposed the main damping source on bearing. Squeeze film effect due to approaching rolling bodies, oil shearing between the rolling elements and raceways and cage-roller relations are possible damping mechanisms.

Lubricants are important to reduce friction and wear on conformal and non-conformal surfaces, and they provide damping within the contact area. Rolling bearings have limited

lubrication area and carry high loads in radial directions. Therefore, the contact surfaces do not conform well to each other. Elastohydrodynamic lubrication (EHL) is a type of fluid film lubrication that exist in non-conformal machine elements, such as bearings, gears, cams and followers. When a bearing operates under radial load, the actions of the regions differ due to traction in the load zone. Therefore, loaded and unloaded areas behave differently. Furthermore, lubricant types and amounts (fully flooded, starved) are decisive for contact characteristics [17].

The area of the rolling contact can be divided into three regions under EHL conditions. EHL damping is dominant in inlet region. Due to increasing pressure in the middle zone, Hertzian stiffness has major effect. Damping is negligible in exit region because of the releasing pressure. Figure 2.6 and Figure 2.7 show the dynamic characteristics of roller-raceway EHL contacts.

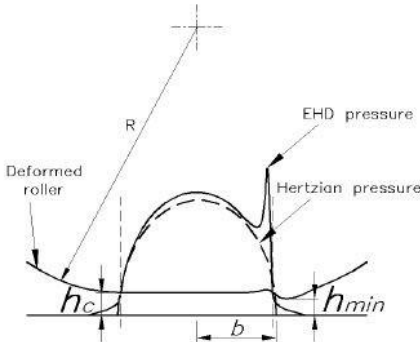


Figure 2.6. EHL in line contact from [5]

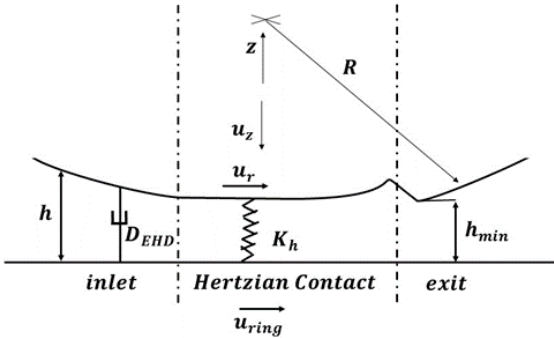


Figure 2.7. Damping and Stiffness in EHL from [5]

EHL problems are governing with Reynolds, rheology and elasticity equations [18]. One way of the determining damping forces in EHL problems is Computational fluid dynamic (CFD) approach. CFD solution is used the whole Navier-Stokes equations, which is given in Equation 2.18 [19]. Navier-Stokes equations includes gravitational, pressure and

viscous forces. It uses for Newtonian fluids. CFD considers both solid and lubricant damping. It's an iterative method, therefore it may cause time-consuming processes.

$$\rho \frac{Du}{Dt} = \frac{\partial p}{\partial x} + \text{div}(\mu \text{ grad } u) + S_{Mx} \quad (18)$$

$$\rho \frac{Dv}{Dt} = \frac{\partial p}{\partial y} + \text{div}(\mu \text{ grad } v) + S_{My} \quad (19)$$

$$\rho \frac{Dw}{Dt} = \frac{\partial p}{\partial z} + \text{div}(\mu \text{ grad } w) + S_{Mz} \quad (20)$$

where, ρ is density, μ is dynamic viscosity; u , v and w are surface velocities for x , y and z dimensions, respectively; S_{Mx} , S_{My} and S_{Mz} are the momentum terms for three dimensions (x, y, z).

Reynolds Equation uses to solve Navier-Stokes equation as well. Reynolds equations is only applicable for Newtonian fluids and thin film lubrications. It's valid for too high contact length and thickness ratio (length/thickness $\gg 1$). There is no temperature difference in contact direction. Pressure is constant in a straight line of the bearing radial direction, as shown in Figure 2.8. Oil inertia is neglected.

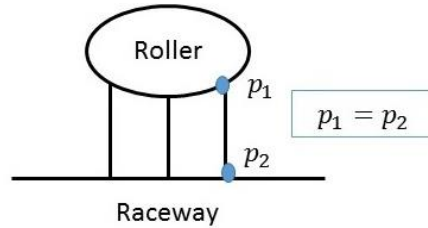


Figure 2.8. Pressure assumption in Reynolds Equation

Reynolds equation is a non-linear differential equation, so that the analytical solution is just possible under some assumptions [20]. An analytic solution for Reynolds equation and assumptions are given below.

1. Side leakages from the contact is ignored.
2. The clearance for contact partners is defined with the parabolic curve given by [20].
3. Minimum oil film thickness is larger than the surface roughness.
4. Inertia forces are smaller than the viscous forces.
5. Gravitational effects are ignored.
6. Viscosity assumed constant.
7. Cavitation does not cause any negative pressure.

By means of these assumptions, Reynolds equation is integrable and the force by entry zone is:

$$P_e = \frac{2\eta URL}{h_0} + \frac{3}{\sqrt{2}} \frac{\pi V \eta R^{1.5} L}{h_0^{1.5}} \quad (21)$$

where, η is oil viscosity, U is rolling speed, L is length of the contact ellipse, R is the conformance, h_0 is central film thickness and V is approaching velocity. The right hand-side of the equation 2.19 has a velocity dependent term. The viscous damping coefficient is considered as,

$$f_e = \frac{3}{\sqrt{2}} \frac{\pi V \eta R^{1.5} L}{h_0^{1.5}} \quad (22)$$

In addition to the above approaches for damping calculations, Dietl has developed an empirical equation to evaluate EHD damping formula [15]. D_{EHD} is a velocity dependent term and it is multiplying with radial approaching velocity between roller and raceway for damping force calculations.

$$D_{EHD} = 10^{-3} K_0 R_x^{K_R} L_{eq}^{K_L} E'^{K_E} \eta_0^{K_\eta} \alpha_p^{K_a} q_D^{K_q} u_\Sigma^{K_u} f_e^{K_f} \quad (23)$$

where, R_x is reduced radius, q_D is load per slice, η_0 is viscosity under air, L_q is contact length, E' is reduced elastic modulus, f_e is inlet zone length factor, u_Σ is sum of surface velocity, and α_p is pressure viscosity coefficient. The coefficients are given in Table 2.1.

Table 2.1. Damping calculation coefficients

K_0	K_R	K_L	K_E	K_η	K_a	K_q	K_u	K_f
0.1963	0.781	0.769	1.069	0.531	0.424	-0.136	-0.434	-0.563
$Kg^{-0.04} m^{0.006} s^{0.0115}$	N/A	N/A	N/A	N/A	N/A	N/A	N/A	N/A

2.2. Multibody Simulation

The main objective of the Multibody simulation (MBS) is to produce a realistic dynamic model of a real system. However, there is a trade-off between model complexity and applicability. As the degree of freedom (DoF) of the model and the number of parameters decreases, the effort in evaluating the results decreases.

A multibody system consists of body elements, constraints and interlinking elements. The components of the system represent physical inertia, elasticity and damping. Rigid bodies consist of mass or inertia in a rigid system. Their masses are assumed to be concentrated on the center of gravity. The spatial position and orientation of the system are stated by a

set of coordinates (Cardan, Euler etc.). The movements of different rigid systems are identified by constraint elements. Constraint elements cause reaction forces when they connect two bodies. Constraints are divided into two groups as time and position dependent elements. Interlinking elements create active forces which depends on the mass, position and orientation of the system. Spring, damper and friction elements are examples of this kind of components [21].

Figure 2.9 shows a multibody system, which includes rigid bodies, constraints and interlinking elements.

To study the motion behaviour, a mathematical model of the system should be derived. The Equation of Motion (EOM) of the system defines the motion of the system. The time dependent equation of a multibody system is defined by [21].

$$M(t)\ddot{x}(t) + P(t)\dot{x}(t) + Q(t)x(t) = h(t) \quad (24)$$

where, $x(t)$, $M(t)$, $P(t)$, $Q(t)$ and $h(t)$ are position vector, inertia matrix, velocity dependent forces, position dependent forces and excitation vector, respectively.

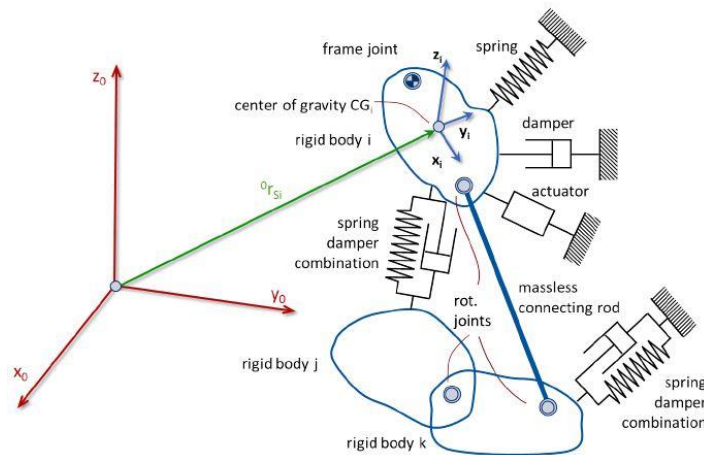


Figure 2.9. A multibody system from [21]

2.2.1. Flexible Body Application in MBS

The MBS approach mainly focuses on rigid body dynamics. However, the rigid body approach may not be efficient to analyse structural systems. Finite element approach is a modelling method which takes the dynamic behaviour of flexible bodies into consideration. The combination of Finite Element Method (FEM) and MBS approaches provide a more realistic description of complex mechanical systems [23]. Figure 2.10 shows a flexible multibody system.

Force elements, constraints and joints creates connecting points (interfaces) between flexible bodies and the other components of the multibody systems. Application of force on these elements cause deformations. Mode shapes indicate the local deformations at connection points, and they represent the eigenmodes of the system [23].

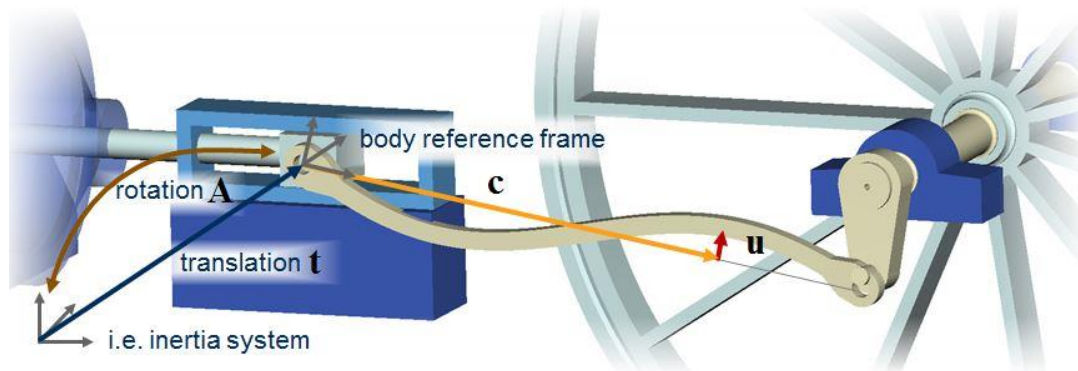


Figure 2.10. A Flexible multibody system (steam engine) from [23]

Rigid bodies are represented by a point placed on their center of gravities while flexible bodies consist of many points which depend on the modelling and analysis requirements. The position of a point of the flexible body is expressed by as [23]:

$$r(c, t) = A(t + c + u(c, t)) \quad (25)$$

where, u is the deformation vector that depends on the location and the time, c is rigid body position according to body reference frame, t is the translation vector, and A is the transformation matrix [23].

Constraint modes consider static deformations, when the body attaches the connection elements at nodes [24]. The constraint modes are obtained for every retained DoF from finite element software. Constraint normal modes are used in high frequency range, in order to examine the natural vibrations of a body when all the connection degrees of freedoms are fixed.

The linear combinations of the constraint and normal constraint modes ensure the final deformation of the integrated elastic elements [23]. The retained degrees of freedom and generalized coordinates of the constraint modes are the coordinates of the integrated element.

Craig Bampton's method is often used to consider elastic bodies in multi-body systems in the previous studies. The method which reduces the size of the flexible model, integrates FEM into the MBS model [25]. The method converts the finite element model into small matrices, which contains the information about mass, stiffness and mode

shapes. The mode shapes are represented in modal or generalized coordinates together with the physical coordinates at the connecting nodes. Although the significant number of nodes of the elastic body is reduced, the reduction still enables an appropriate approximation of the natural frequencies.

Reduction of system DoFs are conducted by,

$$F_{\text{red}} = M_{\text{red}}\ddot{q}_e + C_{\text{red}}\dot{q}_e \quad (26)$$

where M_{red} , C_{red} and q_e are reduced mass and stiffness matrix and selected DoFs respectively [26].

The reduced finite element models can be expressed with the equation given by [23]:

$$M_{\text{SE}}\ddot{u}_{\text{SE}} + D_{\text{SE}}\dot{u}_{\text{SE}} + K_{\text{SE}}u_{\text{SE}} = p_{\text{SE}} \quad (27)$$

where, M_{SE} is the mass matrix, D_{SE} is the damping matrix, K_{SE} is the stiffness matrix, p_{SE} is the load vector and u_{SE} is the deformation vector.

2.2.2. Bearing Modelling in MBS

A rigid multibody system can be defined with bodies and interactions. Bodies are presented by masses, moment of inertias and their body fixed reference frames (BFRF). Force elements, joints and connections are massless modelling elements that provide interaction between model components. Force elements establish applied force and/or torque into the model; joints determine the mechanical degrees of freedom, and connections create kinematic links. Moreover, constraints are used to create additional boundary conditions between two parts. While they perform their duty, they introduce constraint forces and torques in the model. Markers build connection interfaces for different bodies.

Simpack is MBS software, which provides chance to model and analyse mechanical systems in simulation environment. In Simpack, bearings are modelled as force elements. An input is delivered to bearing inner ring and this output is transmitted to housing through bearing. The difference between the input and the output is determined by the bearing dynamics. In MBS, three different approaches can be used to model bearings.

One of the methods of the bearing modelling in MBS is using pre-calculated stiffness and synthetic damping parameters (namely characteristic models). In Simpack, the two force elements, such as bushing element and spring-damper element, can be used to obtain radial contact forces between rollers and raceways. While bushing elements apply forces

and torques in x, y, z directions, spring elements apply only forces in x, y, z directions, as outputs. The bushing and spring elements use constant stiffness and damping values as parameter. If only one bushing or spring element is applied between inner and outer ring, the model may not be realistic enough, since the contact forces between each roller and raceway are not considered. This kind of models do not include any EHD calculations and mainly have constant parameters for stiffness and damping forces. Therefore, they can't reflect the non-linear properties of the bearings.

Some of MBS software have inherent bearing models are called benchmark models. For instance, Simpack has its own bearing model, which is called Rolling Bearing. Rolling Bearing uses bearing geometrical properties. It uses bearing components, and the contact forces are determined with Hertzian calculations. EHD contact relations neglected in the model [23]. The benchmark models also contain synthetic damping parameters.

The third approach of the bearing modelling in literature is based on user-defined elements, namely, subroutines. Some of the MBS software provides opportunities for users to create their own calculations. Due to its complex structure, the bearing itself is considered as a multi-body system. While rings, rollers and cage are created as bodies, contact forces are determined with force elements. In the literature, various bearing models are developed for MBS software. Fritz [27], Teutsch [1] and Qian [5] have developed their own models. All of the models are generated using bearing components, and they have detailed bearing force calculations. These models also have employed Hertzian approach for contact stiffness calculation and EHL approach for contact damping and friction calculations. However, the effect of the EHD contact on stiffness calculations are neglected.

Multibody simulation results can be analysed in frequency domain. The modal analysis and linear system analysis are useful tools for frequency analysis in Simpack. The modal analysis fundamentals are explained in Section 2.3.

2.3. Modal Analysis

2.3.1. Numerical Approach

In vibration analysis, mechanical systems can be classified using three different mathematical models. One of these models, known as "spatial model", is made up from the spatial properties of the system. The model includes mass, stiffness and damping properties as matrix forms, and it can be represented by equation [2.22] [28].

Another model is derived from free vibration analysis using Equation [2.22] ($h(t) = 0$), and called "modal model". With the analysis, N natural frequencies and N damping values are obtained, and these terms are associated with mode shape vectors of the system. Each specific natural frequency and damping value corresponds to a mode shape. The solution of the modal model includes two matrices, $[\lambda^2]$, $[\Phi]$. These two matrices are referred to as modal properties (eigenvalues) and eigenvectors. The matrix $[\lambda^2]$ is a diagonal matrix and one diagonal element of the matrix contains natural frequency and the damping factor for the related normal mode of vibration. The corresponding column of the matrix $[\Phi]$ represents the shape of the same mode of vibration [28].

The third model is obtained from forced vibration analysis, and known as "response model". When an excitation force is applied to a mechanical system, the solution of equation of the motion can be described by a single matrix, which is called "The Frequency Response Matrix" $[H(w)]$. Although the first two models have constant parameters as elements of the matrices, the elements of frequency response matrix is frequency dependent, and each of these elements is a Frequency Response Function (FRF). For each of the FRF, the elements of frequency response matrix is written by [28]:

$$H_{jk}(w) = \frac{X_j}{F_k} = \sum_{r=1}^N \frac{rA_{jk}}{\lambda_r^2 - w^2} \quad (28)$$

The first term on the right-hand side of the equation [2.26] is written by spatial properties. While X_j represents the vibration response of the j^{th} DoF, an excitation force is applied on the other DoF k . The latter expressions on the right-hand side shows the FRF with modal properties. In the expression, λ_r^2 is the eigenvalues of r^{th} mode, rA_{jk} is constructed from r^{th} eigenvector, and is called the modal constant and N is the number of DoF. The second expressions give a direct relation between modal properties of a system and its response behaviour.

2.3.2. Linear System Analysis

Mechanical systems are represented in simulation environments via their mathematical models. The detailed and realistic descriptions of mathematical models are generally non-linear, and valid for large motions. In dealing with mathematical models, they are mainly represented by differential equations, which can be linearized to less complex and first order equations. A linearized model is only valid for infinitesimal neighbourhood of the reference motion.

In order to integrate the linearized EOM in MBS environment for numerical calculations, mathematical model is inverted in state space form. State Space Matrix (SSM) form represents the system dynamic behaviour, and by means of SSM 2nd order differential equation model (EOM) is converted to 1st order model. The SSM form of linearized system EOM in time domain shown below:

$$\dot{x}(t) = Ax(t) + Bu(t) \quad (29)$$

$$y(t) = Cx(t) + Du(t) \quad (30)$$

where; x is the state vector, A is the system matrix, B is the input matrix, t is the model time, u is input vector, C is the output matrix, D is the feedforward matrix and y is the output vector. While matrix A includes system dynamic parameters, it provides the eigen-characteristics of the system. The state vector x includes information about positions and velocities of independent states, and y contains set of quantities to be measured [23].

The SSM is transferred to frequency domain in order to obtain the FRF of the system. The frequency domain representation of SSM is given by:

$$j\omega I \hat{x}(j\omega) = A \hat{x}(j\omega) + B \hat{u}(j\omega) \quad (31)$$

$$\hat{y}(j\omega) = C \hat{x}(j\omega) + D \hat{u}(j\omega) \quad (32)$$

where I is the identity matrix. When the above equations are solved by y as a function of u ,

$$\hat{y}(\hat{u}) = [C(j\omega I - A)^{-1}B + D] \hat{u} = H(j\omega) \hat{u} \quad (33)$$

the single transfer functions of the systems are

$$H_{io}(j\omega_k) = \frac{y_o(j\omega_k)}{u_i(j\omega_k)} \quad (34)$$

In Simpack, the above equation separates magnitude, phase and output for each discrete frequency k using LSA [23].

2.3.3. Experimental Approach

The main objective of the experimental modal analysis is to obtain the modal parameters of a structure experimentally. At the beginning of the experimental modal testing, a series of FRFs are measured and then the modal parameters are extracted during the post process. Specific modal parameters, which are the eigenfrequency (ω_r), modal damping (η_r) and the modal constant (rA_{jk}), can be estimated from a single FRF [29]. A series of FRFs can be measured by either varying the excitation or sensing position.

Free support is used to determine the eigenmodes in free conditions. Free condition means that the test object is not connected to any points of the ground. In practice, a very soft spring, such as light elastic band, is used to provide free conditions. Rigid body modes, mass and inertia properties are generally obtained by free supports. There are various options for the excitation forces. Excitation forces can be continuous (sinusoidal, random) or transient (impulse) [28]. For transient excitation, the structure can be excited in wide frequency range by a hammer, and the force at the hammer is measured. Although reproduce ability is a problem of the hammer test, flexibility and ease of use are the advantages of hammer test.

Test signals are digitalized by using measured signal in sampling process. If the sampling rate is too small, the existence of the high frequency signals may be overlooked, and this situation is called aliasing. A digital signal processing method, which is called Shannon's Theorem, is used to obtain suitable sampling frequency of a signal. According to Shannon's Theorem, sampling frequency should be more than two times of the maximum frequency of the signal. Figure 2.11 shows the relation between the Shannon's theorem and aliasing [30].

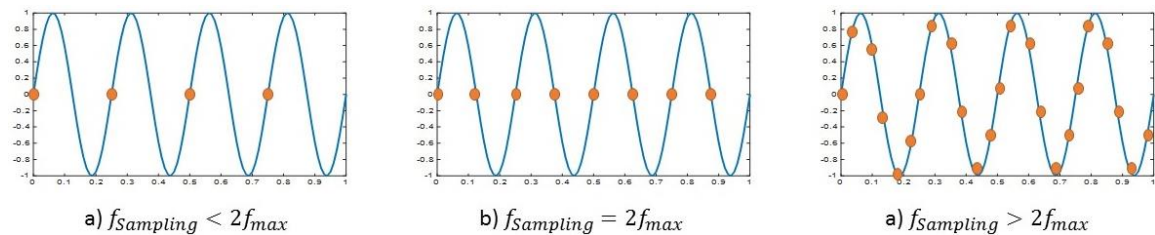


Figure 2.11. Aliasing and Shannon's Theorem, adapted from [30]

In practice, for one input of the Frequency response matrix, more than one frequency response functions are measured and an average value is calculated to get rid of the external effects. Coherence is a quantity between 0 and 1, and it is used to compare the FRFs. When the coherence is 1, the excitation can be computed exactly and when coherence is 0, the signal is completely noisy. The coherence is determined by Equation [2.33]. The details can be found in [31].

$$\gamma^2 = \frac{|G_{XF}(w)|^2}{G_{XX}(w)G_{FF}(w)} \quad (35)$$

For obtaining relation between analytical and experimental FRFs, curve fitting processes are performed. In the literature, there exist a large number of curve fitting methods. The details of the methods can be examined in [28]. One of these methods, Rational Fraction

Polynomial Method (RFP), is explained here. RFP is a multi-DoF modal analysis approach, and it can create a curve fit for the corresponding eigenmodes. RFP is called the global RFP when more than one FRPs are analysed. The analytical FRF can be obtained by [29].

$$H(w) = \sum_{r=1}^N \frac{A_r}{(w_r^2 - w^2 + 2iww_r\zeta_r)} \quad (36)$$

where, A_r is the modal constant, w_r the eigenfrequency and ζ_r is the modal damping. Equation [2.34] can be written as a polynomial using polynomial coefficients,

$$H(w) = \frac{(b_0 + b_1(iw) + b_2(iw)^2 + \dots + b_{2N-1}(iw)^{2N-1})}{(a_0 + a_1(iw) + a_2(iw)^2 + \dots + a_{2N}(iw)^{2N})} \quad (37)$$

2.4. Case Study on Bearing Contact Dynamics

Up to this section, the fundamentals of the bearing dynamics, MBS and the modal analysis are presented. In this part of the study, a rigid shaft bearing system is used to examine the basic differences of the various bearing contact models. For this aim, a bearing model is built in Simpack environment, and three contact models (Hertz, CFD and Reynolds) are implemented.

In this section, the model building process of a cylindrical roller bearing is explained. N1014 type bearing is selected, and the geometric and material properties of the bearing is presented in Table 2.2.

The bearing is modelled as a multibody system. For this purpose, inner ring, outer ring and rollers are created separately. There is no cage geometry in the model since the cage and the other bearing components contacts are out of interest. Instead of creating geometry, one center and 24 pocket markers are created to represent rigid cage. Pocket markers are related with rollers, and each roller is matched with one pocket marker. Pocket markers placed on the pitch circle with equal distance. At the beginning of the simulations inner ring, outer ring and cage center markers are on the same point, which is called bearing center.

Table 2.2. Properties of N1014 Cylindrical Roller Bearing

Cylindrical Roller Bearing N1014	
Bore Diameter	70 mm
Inner Raceway Diameter	82 mm
Outer Raceway Diameter	100 mm
Bearing Outer Diameter	110 mm
Thickness	20 mm

Roller Diameter	9 mm
Roller Length	9 mm
Diametral Clearance	0 mm
Number of Rolling Elements	24
Material	Steel
Density	7850 kg/m ³
Young Modulus	210000 MPa
Poisson Ratio	0.3

This study focuses on the radial forces. Therefore, all the other contact forces are not considered here. DoFs of the parts are determined accordingly. Cylindrical roller bearings have low axial load carrying capacities, hence translational movements along x direction is prevented for all parts. While inner ring has 3 rotational DoF and 2 translational DoFs, outer ring can only translate 2 directions (rotational DoFs neglected). The cage can only rotate about x-axis of the bearing center. Cage rotation about x axis is independent from inner ring rotations, and other DoFs are prevented. Rollers and cage pocket markers are connected, and they can rotate with cage center. Rollers have a translational DoF with respect to cage pockets on their y-axis (radial directions). The created bearing model on Simpack is shown in Figure 2.12.

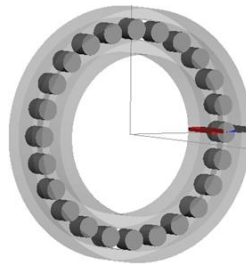


Figure 2.12. N1014 bearing model in Simpack

Two types of force elements are built for modelling of the bearing contact forces. Force Element Rolling Bearing (FE88), as the state-of-the-art model, is used to validate developed models. Bushing elements are used to form contact interactions between rollers/inner ring and rollers/outer ring. Bushing elements have stiffness and damping values for all the translational and rotational DOFs. Only translational y direction components of stiffness and damping are considered for radial force calculations. The elements are created for each contact region. Thus, the bearing model includes 48 force elements for contacts.

Bearing contact force interactions are formed using three different methods. One of these methods is Hertz contact model. Hertz contact stiffness calculation is presented in

Equation [2.36] and [2.37] [3]. It is worth mentioning that there is no damping term in Hertz calculations.

$$\delta = 3.84 \times \frac{10^{-5}Q^{0.9}}{1^{0.8}} \quad (38)$$

$$F = k\delta \quad (39)$$

FEM is another technique to calculate Hertzian contact stiffness. In this study, contact stiffness is calculated using Abaqus.

Reynolds and CFD models are obtained by MSE Tribology Department [2]. Reynolds equation is conducted according to assumptions in chapter 2.1.7.2. CFD results are calculated numerically using software Open Foam [2]. Both solid and fluid contact properties are taken into account for calculation. The middle region of the contact zone are used to obtain stiffness and damping values. The simulations are performed for each node of the fluid and solid. The working flow of the CFD simulations are given in Figure 2.13. While a pressure map is using the fluid–solid interactions, Abaqus co-simulations are performed for Solid Finite Element (FE) calculations.



Figure 2.13. The work flow of the CFD simulations

To obtain stiffness and damping parameters of the CFD model, the operational conditions of the case are selected as in Table 2.3.

Table 2.3. Obtained CFD Models Operational Conditions

Slice width(mm)	Force (N)	Velocity (m/s)	Temperature (°C)
0.45	40	3	40

CFD Simulations are performing for a roller and a ring. The roller divided 20 slices and 1 slice has 0.45 mm length. The force calculations are conducting for a slice to avoid high computation efforts. Static force (40 N) is applied and the slice and bearing has 3 m/s velocity, which called cage linear velocity in literature. Bearing temperature (40°C) is assumed constant. The obtained parameters are given in Table 2.4.

Table 2.4. Bearing Contact Parameters for Various Contact Models

Calculation Method	Stiffness (N/m)	Damping (Ns/m)
CFD	1.8×10^7	15
Reynolds	1.49×10^7	24
Hertz	2.1×10^7	-

A shaft bearing model is developed to perform rigid body simulations. The model contains a shaft and a bearing, which is modelled previously. The bearing is placed in the center of the shaft. The translation in axial direction is prevented for all components. Inner ring and shaft are connected to each other with a zero DoF joint. They can translate and rotate together on 5 DoFs. A housing marker is created, and it is fixed to the ground. Outer ring has 2 translational DoFs (y and z), and it is connected to housing marker with a force element. 40 N preload applied between inner and outer rings. Figure 2.14 and Figure 2.15 show, the system in MBS environment and element interactions of the shaft-bearing system, respectively.

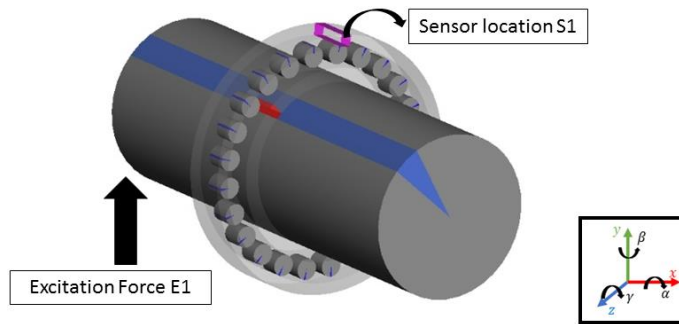


Figure 2.14. Rigid shaft bearing system

A constant force 60 N is applied in radial direction (y) on the shaft BRF. A sensor is created to obtain the acceleration difference between housing and outer ring BRFs. This system is built for Hertz, FE88, CFD and Reynolds models.

The results are analysed using Linear System Analysis via Simpack. LSA determines transfer functions of the linearized MBS model, and responses of the system represented in frequency domain. LSA also uses state-space matrices formulation of the equations of motion, therefore the non-linearities of the system isn't considered. Hertz, FE88, Reynolds and CFD contact models are applied to system separately and LSA results of the systems are compared each other.

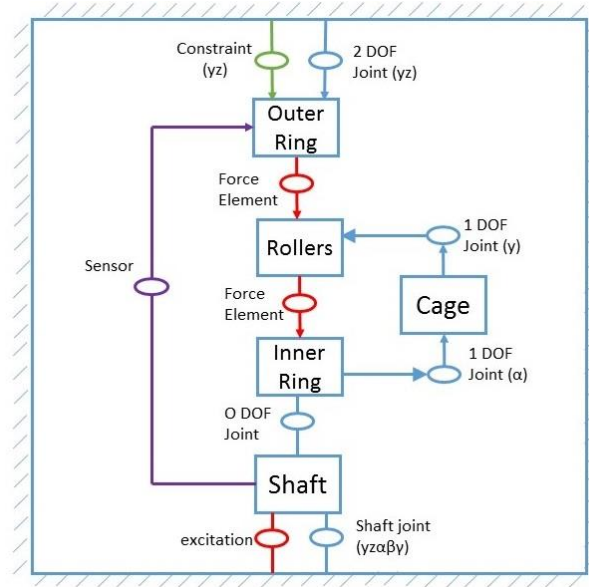


Figure 2.15. Shaft and bearing interaction in 2D representation

Single bearing simulation results are presented in Figure 2.16. According to results in Figure 2.16, two resonant peaks are observed for each model. Resonances represent same modes of simulation model. The first peak belongs to the shaft radial translational movement (on y-z plane), and the second peak represents the outer ring translational movement (on y-z plane). Simpack intrinsic model Rolling Bearing and discrete data Hertzian model have almost the same dynamic behaviours for both modes. The magnitudes and eigenfrequencies are quite similar. Both two model uses Hertzian contact approach, and the results show the modelling approach is supposed to be valid. Figure 2.17 shows a zoomed plot around the first peak in Figure 2.16.

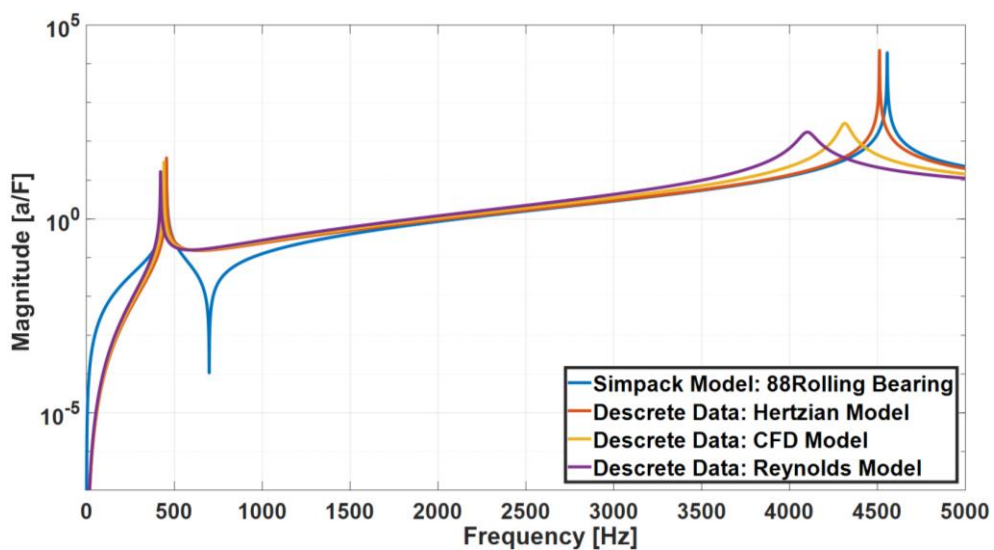


Figure 2.16. LSA Comparison of discrete data models w.r.t. Excitation E1 and Sensor S1

S1

According to Figure 2.17, Hertzian contact model and Roller Bearing model matches well, and their eigenvalues are the same. Since CFD model has higher stiffness with respect to Reynolds model, the first resonant peak is observed larger frequency. Hertzian model has largest eigenvalue due to highest stiffness. While Hertzian and Rolling bearing models have no damping, CFD and Reynolds models have damping parameters. Therefore, EHD based models have smaller magnitudes than Hertzian based models.

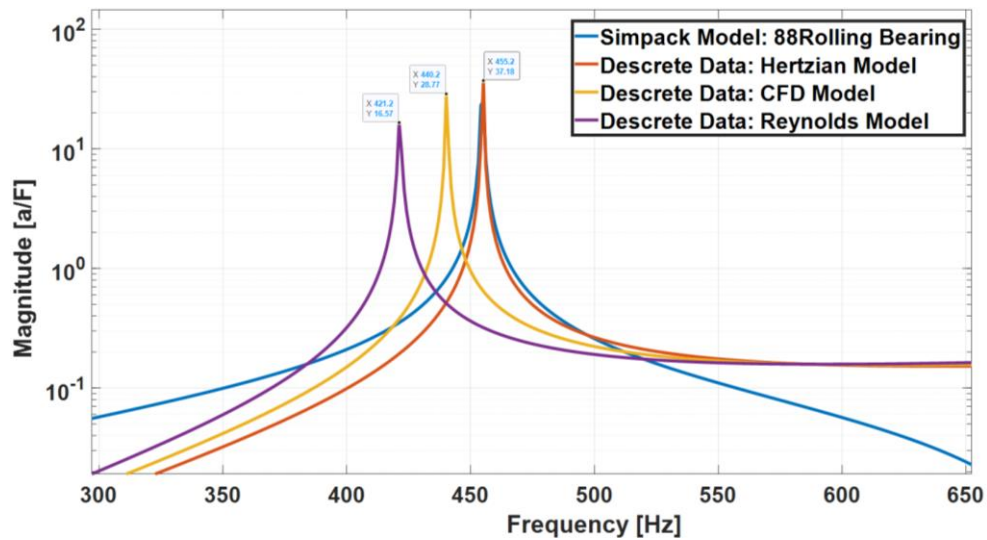


Figure 2.17. Zoomed version of Figure 2.16

The case study shows, bearing contact modelling approach has an impact on shaft bearing model transfer function. For more detailed investigation, EHD and Hertzian based continues bearing models are developed using Simpack subroutines. To investigate the effect of bearing model on mechanical systems, flexible shaft-bearing system models and a flexible gearbox model are built, and eMBS analyses conducting using these models in following chapters.

3. DYNAMIC MODELLING OF CYLINDRICAL ROLLER BEARING

The fundamental of bearing dynamics, MBS and model analysis are explained in Chapter 2. The case study presented in the previous chapter shows how the contact modelling method may change the total bearing transfer path.

The detailed bearing models provide more realistic results, and the effects of the models can be examined in details. There are translational and tangential forces and moments between bearing elements, which are shown in Figure 3.1. Roller-raceway, cage-roller, roller-edge (in axial direction and roller-rib contact forces are contact forces in a rolling bearing [32].

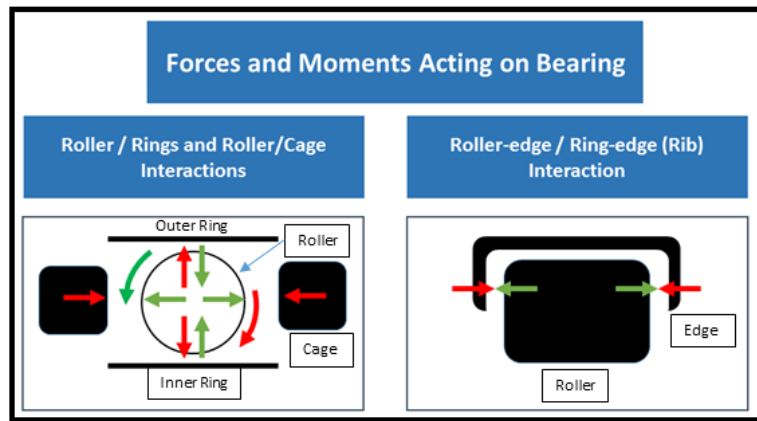


Figure 3.1: Forces and moments inside a bearing

In the current study, only radial forces are considered, as other forces and interactions are considered as out of scope. A new bearing contact force model is developed using MBS software Simpack. At first, Hertzian contact force calculation approach is used as a basis model, and the model is then extended to a CFD-based EHD contact model. The work flow of the developed model is shown Figure 3.2.

The developed dynamic model starts by calculating the roller profile. Then contact detection algorithm is conducted. The algorithm uses similar approach as in [27] to avoid time-consuming calculations. The contact detection is determined using four different aspects. Radial displacement, tilting, roller profile and radial clearance are taken into account. In contact detection process rollers are divided into slices and slice forces are calculated accordingly. The tilting angle is obtained directly using Simpack Access Function. Access Functions provide chance to transfer information between Simpack and subroutine for each time step. The information can be velocity, position, angle,

acceleration, force, torque etc. The model performs contact stiffness calculations using load-deflection relationships. The load distribution of the bearing is considered for stiffness and damping calculations.

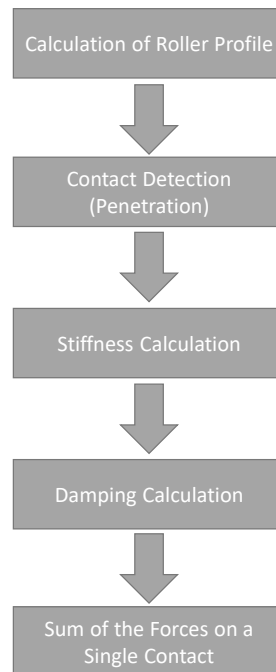


Figure 3.2. The developed model flow chart for contact force calculations

The new model is developed as an open-source program. It has a modular structure and every step of the model flow has its own substructure. The subprograms are formed for this aim. The model avoids hard-coding and can decrease computation time. Simpack is used to build the new model, and details are presented in this chapter.

3.1. Model Development in Simpack

Simpack gives an opportunity for its users to create their user-defined-force-elements, in short User-Force (UF). Force elements are massless modelling parts that provide interaction between system components. They establish applied force and/or torque in the model. User routines of Simpack is operated by users, in order to develop a user-defined force elements. FORTRAN programming language is used in subroutines [23]. In this study a new user-force is developed to calculate the roller-raceway contact forces. Two contact force calculation models are developed in the study. The first model, which is, namely Hertzian model, uses Hertzian contact calculations and it is created as a basis for EHD contact calculation model, namely EHD model. Hertzian model is created in order to validate modelling approach, and Simpack Model 88 Rolling Bearing is selected as a reference of Hertzian model. However, thanks to its modular and open-source structure,

it is changed to other contact calculation model obtained from EHD calculations. Figure 3.3 shows the flow chart of developed model.

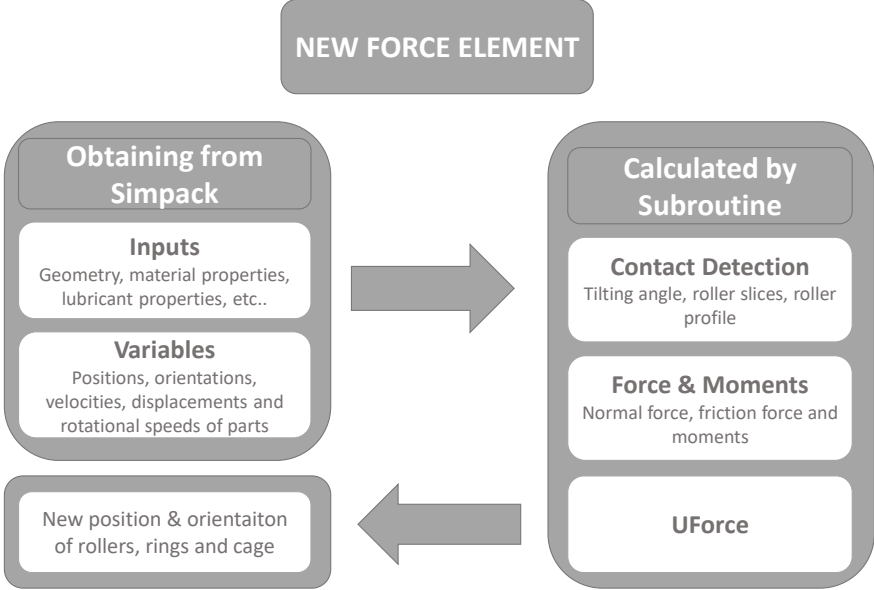


Figure 3.3. System flow chart for User-Force

In the beginning of the calculation process the user defined parameters are taken from created Simpack user interface. The positions and orientations of rollers, rings and cage are read from Simpack using body fixed reference frames (BFRFs), synchronously. Simpack Access Functions provide direct connection to model parameters from MBS model [23]. From position and orientation information; translational velocities, rotational speeds and displacements are obtained as well. Then, the contact force calculations are conducted with mathematical expressions within the subroutine. Finally, obtained force information are transferred back to Simpack for time integration. These calculations are repeated for every time step separately. The details of the modelling process is explained in following parts of the chapter.

3.2. Modelling of Bearing Kinematics

3.2.1. Position and Orientation of Rings

Inner and outer rings are assumed as rigid bodies therefore the inertia and position of these bodies are used in equation of motion of the system. Bodies have body fixed reference frames on their geometric center in Simpack. The positions and velocities of the rings can be obtained from body fixed reference frames [BFRF]. The contact forces between rings and rollers source from the deformation of the components, and it is

determined by a new force element. The acquired three-dimensional forces and moments are placed on the BFRFs [23].

Inner ring position and orientation is defined with respect to outer ring coordinates. The distance between the rings are obtained from Simpack as matrix (\underline{s}), and the orientation of the inner ring according to outer ring is read using Euler angles. Inertia effects of the bearing parts are ignored, since bearing is assumed to move at low speed [27]. Figure 3.4 shows positions and orientations of the rings.

It is assumed that y and z axes are used for radial directions and x is used for axial direction. The displacement and force calculations are governed with cylindrical coordinates (s_{rad}, s_{ax}, ϕ_s), which can be defined as three dimensional coordinates. The axial (s_{ax}) and radial displacements (s_{rad}) are given by [27]:

$$s_{ax} = s_x \quad (40)$$

$$s_{rad} = \sqrt{s_y^2 + s_z^2} \quad (41)$$

The load direction (ϕ_s) is calculated by:

$$\phi_s = \arctan\left(\frac{s_z}{s_y}\right) \quad (42)$$

The coordinates s_x, s_y, s_z are obtained by Simpack Access Functions.

According to Euler sequence, the system rotates with the order of z axis, x axis and new x axis. The angles are referred by ψ (z axis), ϑ (x axis) and φ (new z axis). The results of Euler sequence given by [23]:

$$A_{14}^{(\gamma-\alpha-\gamma)}(\psi, \vartheta, \varphi) = A_{12}^{(\gamma)}(\psi)A_{23}^{(\alpha)}(\vartheta)A_{34}^{(\gamma)}(\varphi) \quad (43)$$

$$A_{14}^{(\gamma-\alpha-\gamma)}(\psi, \vartheta, \varphi) = \begin{bmatrix} c\psi c\varphi - s\psi c\vartheta s\varphi & -c\psi s\varphi - s\psi c\vartheta c\varphi & s\psi s\vartheta \\ s\psi c\varphi + c\psi c\vartheta s\varphi & -s\psi s\varphi + c\psi c\vartheta c\varphi & -c\psi s\vartheta \\ s\vartheta s\varphi & s\vartheta c\varphi & c\vartheta \end{bmatrix} \quad (44)$$

The tilting angle (θ) is obtained by the angle of x_i and x_o (in Figure 3.4) via direction cosines [27]:

$$\theta = \arccos[\cos\psi \cos\varphi - \sin\psi \cos\vartheta \sin\varphi] \quad (45)$$

where ψ, ϑ and φ are Euler angles.

In addition to the tilting of the two directions (around y and z axis), there still exists a third direction of rotation which is the rotation of inner ring around the bearing axial direction. The angle ϕ_{IR} is a result of the rotation of the inner ring about the x_o axis of

outer ring. For small tilting angles Euler angles can be used to calculate ϕ_{IR} . The angle is determined by the angle of y_i and y_o (in Figure 3.4) via direction cosines [27]:

$$\phi_{IR} = \arccos[-\sin\psi\sin\varphi + \cos\psi\cos\theta\cos\varphi] \quad (46)$$

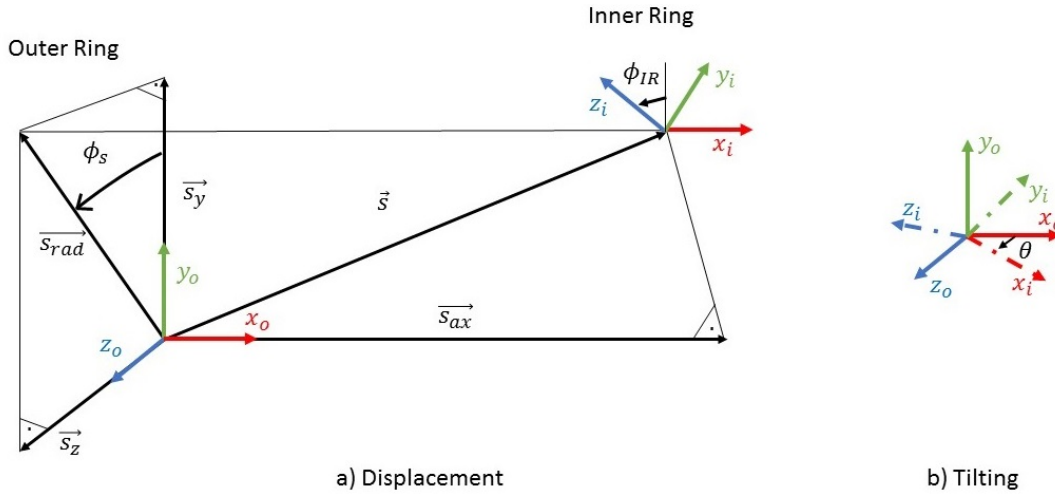


Figure 3.4. Coordinates of inner ring displayed in user routine, adapted from [27]

3.2.2. Position and Orientation of Rolling Elements

The position and orientation of the individual rolling elements can be determined from the position and orientation of the rings. The position of a rolling element in circumferential direction is determined by rolling movement on the rings. Under uniform load and steady state operation conditions, rolling elements slip on raceway can be ignored. The elasticity of the cage is negligible for the circumferential position of the rollers, thus the movements of rollers in cage are not considered in model. With these assumptions the circumferential movements of rollers and cage are supposed to be kinematic [33].

Outer ring is assumed to be stationary and its BFRF is assumed by the reference system. According to Figure 3.5, cage position in circumferential direction is found by [27]:

$$\phi_{cage} = \frac{1}{2}\phi_{IR}(1 - \gamma) \quad (47)$$

The operating pressure, α , differs slightly from the nominal angle (α_0), therefore the nominal pressure angle can be used for calculation of the shaft angle. In roller bearings, rolling elements are equally distributed by circumferential direction, by means of cage. The i^{th} rolling elements position in y-z plane can be found by Equation [3.9].

$$\phi_i \approx \frac{1}{2}\phi_{IR} \left(1 - \frac{D}{d_m} \cos\alpha_0\right) + \frac{2\pi i}{z} \quad (48)$$

where, z is the number of rolling elements.

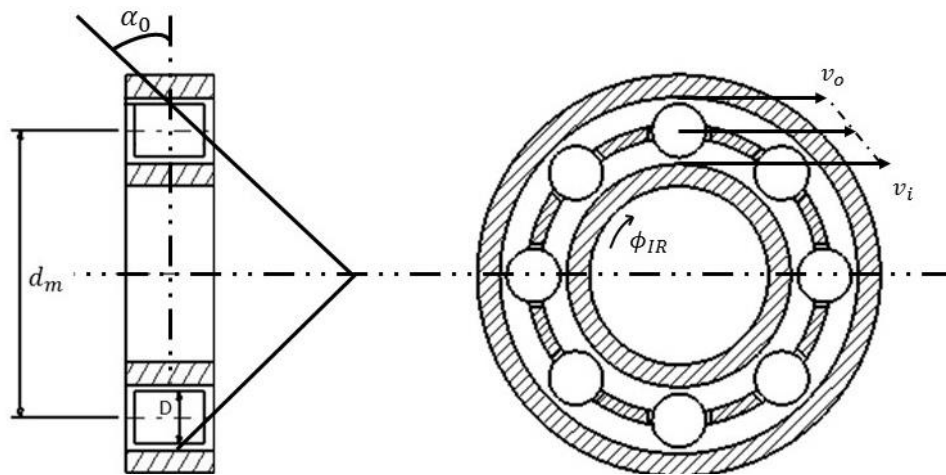


Figure 3.5. Rolling elements movements in circumferential direction, adapted from [27]
 In order to calculate the deflection of contact partners (rolling elements and raceways), rollers are assumed to be located in the centre of the inner and outer raceways. Thus, the radial deflection is regarded as purely geometrical and calculated by geometrical relations. Figure 3.6 shows a possible position of rollers under radial load. According to Figure 3.6, the deflection can be determined from the angle of the rolling element in circumferential direction and the displacement of the rings [27].

$$\phi_{rad,i} = \phi_i - \phi_s \quad (49)$$

The displacements of each rolling elements are determined by:

$$s_{rad,i} = s_{rad} \cos(\phi_{rad,i}) \quad (50)$$

The pitch diameter of bearing is assumed to be retained, and rolling elements are in contact both inner and outer raceways. Therefore, half of the movement of a roller is used as deflection for a roller-raceway contact [27].

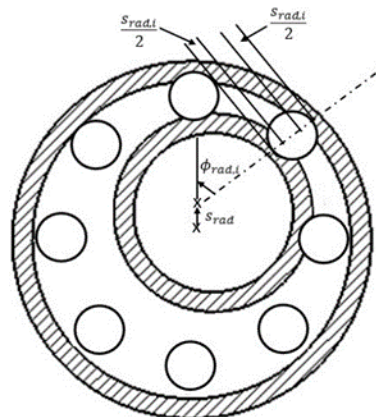


Figure 3.6. Possible roller positions for a radially loaded bearing, adapted from [27]

3.3. Bearing Contact Stiffness Calculation

3.3.1. Applied Load Bearing

The theory of the bearing contact stiffness calculation is explained in chapter 2.1.6. Lundberg equation [8] is chosen in order to model cylindrical roller bearing contact stiffness. The load distribution on a roller is determined using experimentally obtained spring equation [34].

$$Q = c_L \delta^{10/9} \quad (51)$$

$$c_L = 35948L^{8/9} \quad (52)$$

Equation 3.12 is used to calculate the acting load (N) on the rolling element due to deflection (mm) for line contact. In above equations, c_L is supposed to be a stiffness parameter ($N/mm^{10/9}$) and L is the length of the rolling element (mm).

To describe the elastic behavior of a tilted rolling element on a cylindrical raceway, rolling elements are divided into slices along the length direction, and every slice are evaluated separately [6]. Figure 3.7 shows the sliced cylindrical roller geometry.

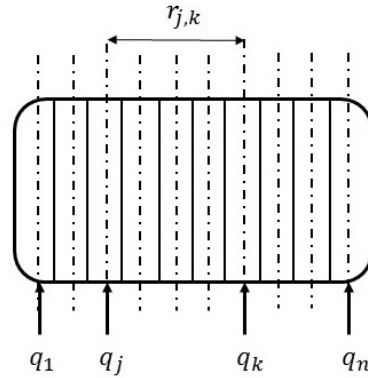


Figure 3.7. Roller geometry with slices

Up to now, one rolling element is considered for load- deflection relationship. The equilibrium forces of the bearing are determined iteratively by computer. The equilibrium conditions for the external forces and moments acting on the ring and the reaction forces of the rolling elements are calculated using Equation 3.14 and 3.15 [34]:

$$F_r - \frac{c_L}{n} \sum_{j=1}^z \left[\cos(\varphi_j) \sum_{k=1}^n \delta_{j,k}^{\frac{1}{9}} \right] = 0 \quad (53)$$

$$M_z - \frac{c_L}{n} \sum_{j=1}^z \left[\cos(\varphi_j) \sum_{k=1}^n x_k \delta_{j,k}^{\frac{1}{9}} \right] = 0 \quad (54)$$

In above equations, F_r is radial force (N), M_z is the moment load on bearing (Nmm), z is the number of rolling elements, n is the number of slices on rolling elements, φ_j is the angular positions of each roller in radial direction (degree) and $q = 9/10$. While Equation 3.14 provides sum of the all forces on bearing, Equation 3.15 gives total moment on bearing.

3.3.2. Contact Detection

The position and orientation of the roller and rings are already described in section 3.2. It is supposed that the rolling element is located in the middle between two rings, and the tilting angle is assumed as half of the calculated tilting angle. Using these assumptions the radial penetration is found by [27]:

$$\delta_j = \frac{s_{rad,i}}{2} + \xi_j \sin\left(\frac{\theta}{2}\right) - c_j \cos\left(\frac{\theta}{2}\right) - \frac{P_d}{4} \quad \text{for } \delta_j > 0 \quad (55)$$

where ξ_j is the distance of each slice to roller mid-plane.

The radial displacement ($s_{rad,i}$), the tilting angle (θ), roller profile (c_j), radial internal clearance (P_d) and for each slice is shown in Figure 3.8.

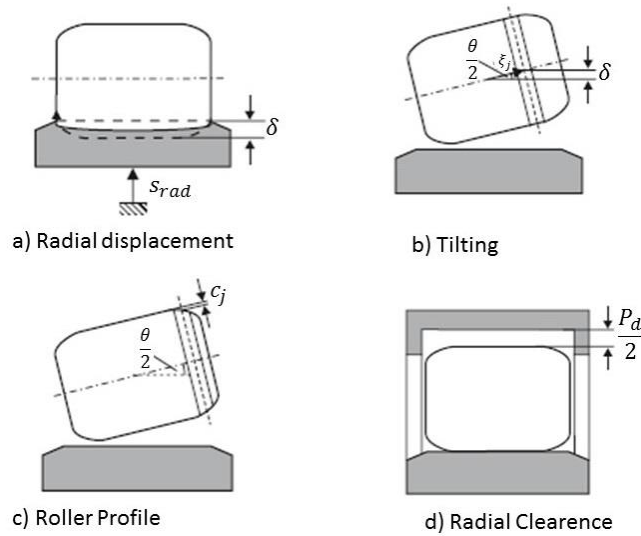


Figure 3.8. Radial Penetration, from [27]

3.4. EHD Bearing Model

The current study focuses on the effect of the different contact force calculation methods on bearing dynamic behaviour. For this reason, two different methods, namely as Hertz and EHD, are considered. Hertz focuses on solid-solid contact interactions, and it is mostly used in contact force calculations in literature. EHD considers fluid-solid

interactions into account, and it includes operational effects, such as velocity, temperature etc. In this chapter, a new rolling bearing model is developed using Hertzian-based model, and the model is considered as a basis for the EHD-based model. CFD approach is used as a calculation method of EHD model. Since CFD simulations need high computation time, they are not feasible to use in the time integration in the MBS. Therefore, pre-calculated stiffness and damping models are used in the developed model. MSE Tribology Department performed CFD simulations and provided the pre-calculated models.[2].The model development process is explained in Section 2.5. NU308 bearing is selected as bearing, and its properties are used to develop CFD model. Both solid and fluid contact properties are considered. Since in the CFD one contact is considered, the same stiffness and damping characteristics are used for roller/inner ring and roller/outer ring calculations. Figure 3.9 shows EHD contact modelling approach.

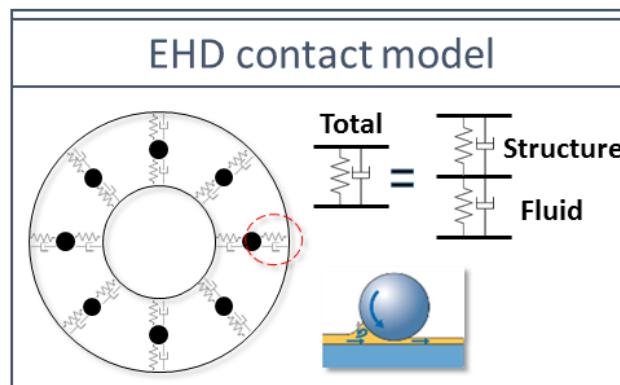


Figure 3.9. EHD Contact Modelling Approach

Open-Foam software is used to conduct CFD calculations. To avoid high computation effort, roller divided into slices. At first one slice-raceway contact is taken into account, and one-slice raceway contact stiffness and damping parameters are calculated. Then this calculation uses to obtain one roller-raceway contact force. This processes are repeated for various load and velocities in order to determine the dependency of stiffness and damping forces on operational parameters. The operational conditions using the simulations are given in Table 3.1. After simulations, the results are used to obtain pre-calculated CFD model. Obtained stiffness and damping parameters are used to calculate roller-raceway contact normal force calculations. While stiffness is multiplied by obtained deflection, damping parameter is multiply by roller-raceway approaching velocity, which is obtained by Simpack Access Function.

Table 3.1. Bearing Properties and Operational Conditions of CFD Simulations

Bearing	NU308
Roller Diameter (mm)	14
Material	Steel
Lubricant	Shell Spirax MA 80W
Simulated Slice Width (mm)	0.7
Simulation Operational Conditions	
Static Force [N]	62
Cage Linear Velocity [m/s]	0.43(500 rpm)-1.7(2000 Rpm)
Temperature [°C]	40

3.5. Validation of Developed Bearing Models

The bearing models are developed using Simpack user routine. A rigid shaft-bearing system is used to validate Hertzian and CFD based models. For that purpose, two developed bearing contact models and Rolling Bearing model in Simpack are implemented on the shaft-bearing system. The system is shown in Figure 3.10.

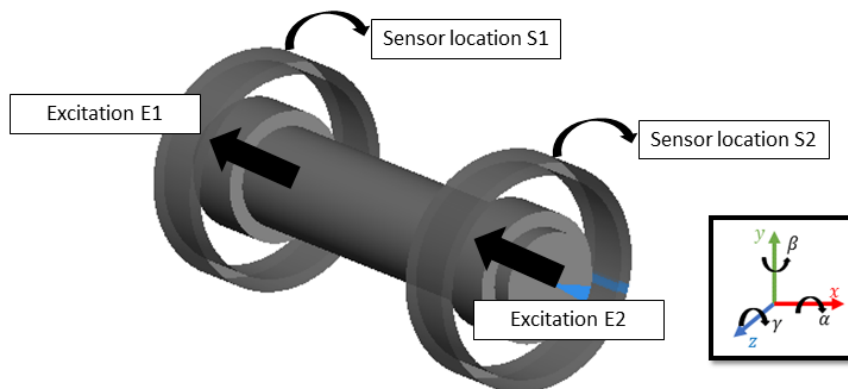


Figure 3.10. Rigid shaft-bearing system in Simpack

Model building process of the system is almost similar to Chapter 2.5, and details of the model building process is presented in there. The model has two bearings, and rollers are not modelled as a body. NU308 type bearing is used, and the geometric and material properties of the bearing is presented in Table 3.2.

During simulations, preload forces are applied on both bearings in radial directions (outer ring to inner ring), which are 100 N in y and 100 N in z directions. Shaft has 500 rpm angular velocity for Hertzian and Rolling Bearing models. CFD model simulations are performed for various cases depends on operational conditions. 500 rpm results of the

CFD model is used in time domain force comparison and LSA comparison. The developed models are built as Force Element (FE), and FE is used to create applied force and torque. The results are obtained using sensor S1, which are located on the outer ring BFRF. The created force inside bearings in y direction is presented in Figure 3.11.

Table 3.2. Properties of NU308 type bearing

Cylindrical Roller Bearing NU308	
Bore Diameter	40 mm
Inner Raceway Diameter	52 mm
Outer Raceway Diameter	80 mm
Bearing Outer Diameter	90 mm
Thickness	23 mm
Roller Diameter	14 mm
Roller Length	15 mm
Diametral Clearance	0
Number of Rolling Elements	12
Material	Steel
Density	7850 kg/m ³
Young Modulus	210000 MPa
Poisson Ratio	0.3

According to the Figure 3.11, both Hertzian and CFD models suit well with the results of Rolling Bearing model. The models are supposed to valid for force generation with respect to time. For deeper investigations of the dynamics of the system, Linear System Analyses are performed.

Hertzian based model is developed using a similar bases used in the Rolling Bearing force element in Simpack. Therefore, the dynamic behaviours of these models should match ideally. The LSA analyses of the models are shown in Figure 3.12. According to the Figure, the dynamic behaviours of these models are quite similar for this system. The first peak of the system represents the system movement (all parts together) in radial direction, and the second peak represents shaft movement in radial direction. The second eigenmode can be considered as a shaft bending mode. While the first peaks of the models

are the same, the second resonances are pretty close. Hertz and Rolling Bearing models have an eigenmodes in 4771 Hz and 4807 Hz, respectively.

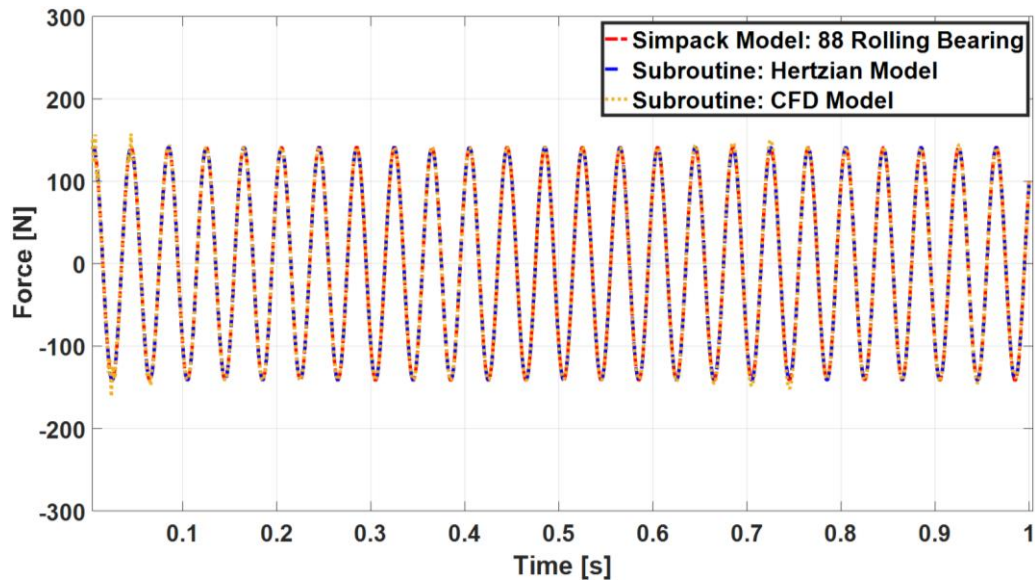


Figure 3.11. Generated Force in bearings in y direction w.r.t. Excitation: E1-E2,
Response: S1

CFD based model uses both fluid and solid interactions for stiffness calculations. According to the case study in Chapter 2.5 and MSE Tribology Department report [2], CFD based model has smaller stiffness with respect to Hertzian based model. The dynamic behaviours of models are almost similar, and the first peaks of models are placed on the same frequency. The shaft bending mode of the CFD based model has smaller magnitude and eigenfrequency, due to different stiffness and damping properties. While Hertzian based model and Rolling Bearing model have no damping effect, CFD based model has damping force. The other reason of differences between eigenfrequencies can be caused from operational conditions of simulations. CFD based model is obtained after 500 rpm, and it is directly affected by the shaft rotational velocity. For lubrication regime under 500 rpm, the available CFD calculations are not valid. For low speed applications, the lubrication regime is mostly affected by mixed lubrication. Since Hertzian based model results are not changing with rotational velocity, only velocity dependent CFD results are examined in here.

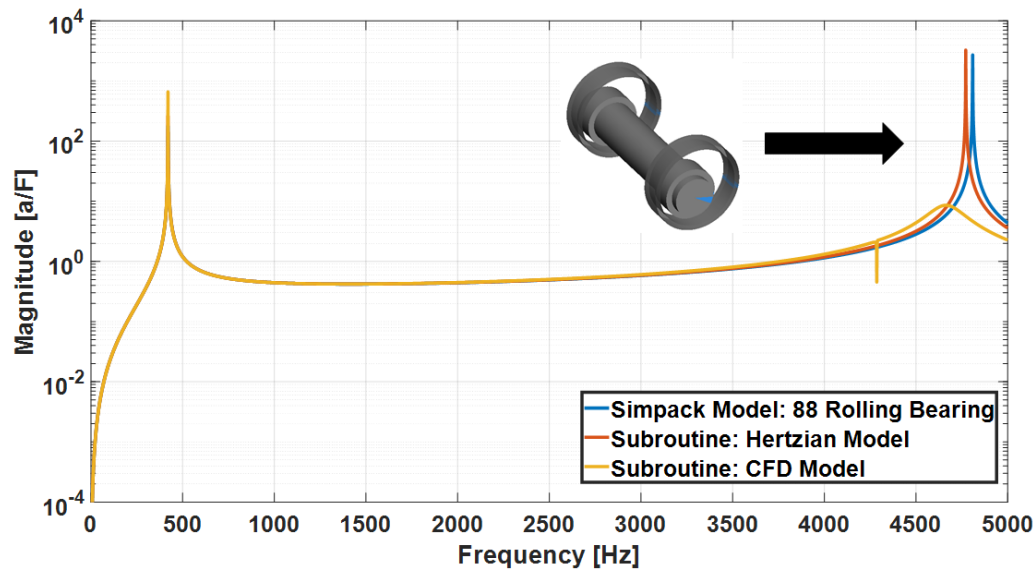


Figure 3.12. LSA comparison of bearing models w.r.t. Excitation: E1-E2, Response: S1
 It is shown in the literature [2] that the dynamic properties of the bearing models should change with operational parameters. While the stiffness and damping parameters of CFD model are decreasing with increasing rotational velocity of shaft (inner ring), the stiffness is increasing and damping is decreasing with increasing applied radial force on bearing.

Figure 3.13 shows LSA results of CFD model for changing shaft rotational velocities. In order to examine the velocity dependency of the model, simulations are performed for 500 rpm, 1000 rpm and 2000 rpm, and 141.2 N force (100 N in y and 100 N in z directions) are applied on both bearings. Results are obtained using sensor S1.

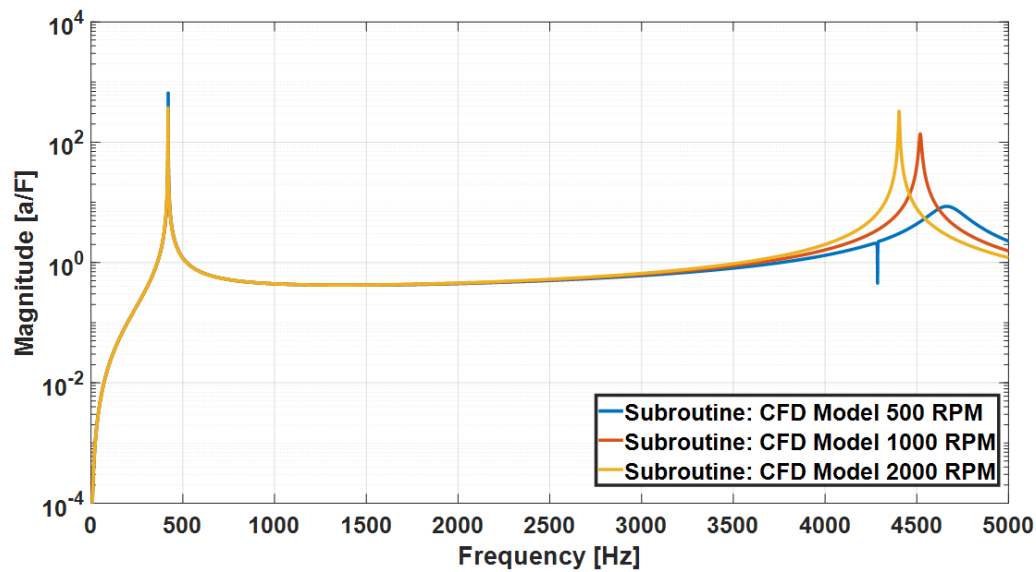


Figure 3.13. LSA of CFD model for various velocities w.r.t. Excitation: E1-E2, Response: S1

According to the results, the first peak is the system movement (all parts together) in radial direction, and the second peak is about shaft movement in radial direction. Both two resonances go to the left due to decreasing stiffnesses, and magnitude of the bending mode is increasing due to decreasing damping. The velocity dependency of the model is observed clearly in the shaft bending mode, and these results fit well with the reference [2].

The frequency response functions of CFD model at various applied force state are presented in Figure 3.14. To investigate the force dependency of the model, simulations are performed for 141.2 N (100 N in y and 100 N in z directions), 212.1 N (150 N in y and 150 N in z directions) and 282.8 N (200 N in y and 200 N in z directions) with 1000 rpm shaft rotational speed. LSA results are obtained using sensor S1.

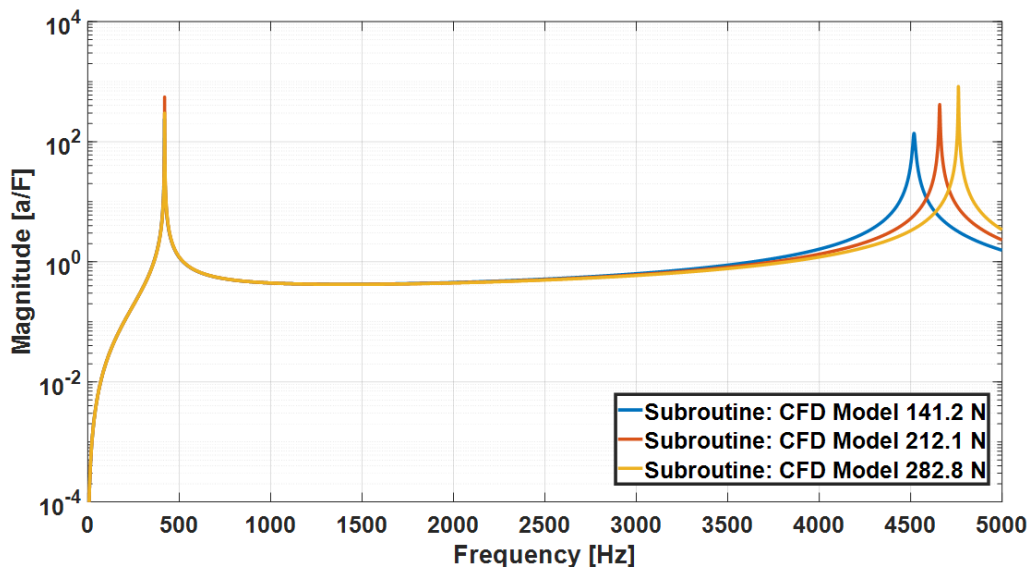


Figure 3.14. LSA of CFD model for various forces w.r.t. Excitation: E1-E2,
Response: S1

The second peak is again related to the shaft bending mode. The mode resonances shift to the right due to increasing stiffnesses, and the magnitude of the bending mode is increasing with decreasing damping. These results suit well with the MSE Tribology Department report [2].

In this chapter, the model development processes of two bearing contact modelling approaches are presented. Hertzian based model is developed to create as platform for the CFD model. After model building process, two models are validated using Simpack intrinsic model 88 Rolling Bearing. The simulations are performed on rigid shaft bearing system, and results are analysed in time and frequency domain. In the next chapter, EHD

and Hertz contact modelling approaches are investigating on flexible systems using the developed models.

4. INVESTIGATIONS ON EHD BASED MODELS

The vibration transfer path of a mechanical system is directly affected by the system components and their dynamic characteristics. The modelling of the system components determines the accuracy of the results. In order to obtain reliable analysis of a system, the component models should be built in details. For this aim, developed bearing models in Chapter 3 are applied on more complex system models in this chapter.

In Chapter 2.5, discrete data contact models are used on a shaft-bearing rigid system. In Chapter 3, two subroutines are created using Hertzian and EHD based contact models, which are used on a shaft-bearing rigid system. In order to investigate the effect of bearing contact models on mechanical systems, elastic multibody simulation (eMBS) approach is used in this chapter. Finite element approach is used to obtain eMBS models, and flexible shaft, bearing and housing systems are built in Abaqus. Bearing models are used as single operating point models (discrete data models) and continuous (subroutine) models in Chapter 4.

4.1. Study on Bearing Testrig: On one single operating point

4.1.1. Modelling and Simulations

To examine the dynamic characteristics of bearing model on flexible shaft-bearing-housing system, one single operating point is used to obtain stiffness and damping parameters. Hertzian and CFD approaches are used to obtain model dynamic parameters. N1014 bearing is selected, and the details of bearing modelling approaches are presented in Chapter 2.5. The operating conditions and model parameters of CFD model are shown in Table 4.1. Similar stiffness and damping parameters in Chapter 2.5 are used for Hertzian model.

Table 4.1. Operating conditions and dynamic parameters of CFD based discrete model.

Operating Conditions of Discrete Bearing Model	
Static Load (N)	15.5
Velocity (m/s)	5.4
Temperature (°C)	30
Model Dynamic Parameters	
Stiffness (N/m)	1.595×10^7
Damping (Ns/m)	13.26

There are two main assemblies of the system, namely shaft and housing. The shaft assembly is shown in Figure 4.1. The assembly consists of a shaft, two rings (as inner ring), two shaft nuts and two bushings. Nuts and bushings are used to stabilize the rings. Boundary conditions (BCs) are used to generate links between Abaqus and Simpack. BCs are transferred as nodes to Simpack, and the nodes can be used to create markers. There are six BCs, which are generated in Abaqus model. Two of the BCs are created for two inner ring center markers. While one of the BCs is composed as external force applying marker, one of the BCs is created as torque applying marker and one BCs for sensor location. The last BC is created for the axial support, and it prevents the axial translation.

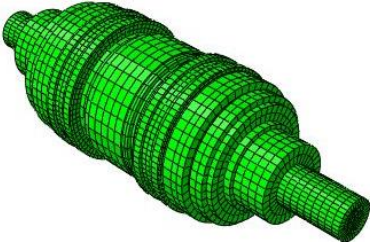


Figure 4.1. Shaft assembly model in Abaqus

The housing assembly is modeled in Abaqus as an elastic body. Figure 4.2 shows the model. It contains, a body as a housing, a base part, two rings as outer rings, bushings as support elements and cover parts. There are two BCs for outer ring centers on center of rings, two BC for sensor locations on body part and four BCs for ground connections on base part.

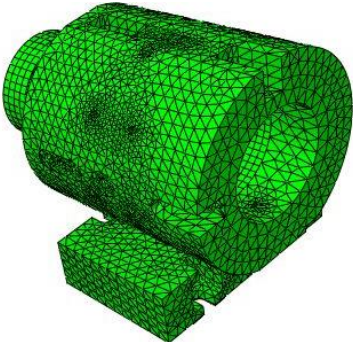


Figure 4.2. Housing assembly model in Abaqus

Two assembly models are imported to the Simpack using Flexible Body Input (FBI) file generator. The details of the model reduction method are given in Section 2.2.1. The generator is used to create flexible model in Simpack. After generating the flexible bodies, markers are created for each BCs. Four markers on the base part fixed to the ground using 0 DoF connection. An external force and excitation torque are applied on the shaft using

two markers. A marker is used to restrain the axial translation movement of the shaft. There are two markers on the sensor location. While one of the marker is moving with the body, the other marker is stationary. These two markers are used to obtain body acceleration differences. The markers on the inner and outer rings are generated to create ring roller contact forces. Contact force models are the same as rigid body approaches. Bearing force elements are directly connected to ring center markers. Figure 4.3 shows eMBS shaft-bearing-housing model in Simpack.

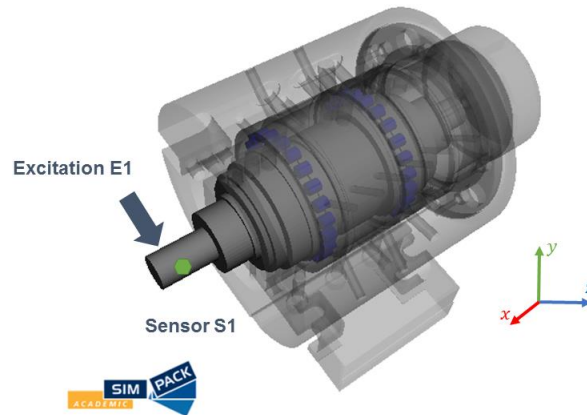


Figure 4.3. Flexible model in Simpack

The simulations are performed with a constant radial force as excitation, and Sensor S1 is used to measure displacement as response (in radial direction z). Three different bearing models are used in simulations, such as Hertzian model without damping, Hertzian model with damping and CFD model. Results are obtained using Linear System Analysis, and Figure 4.4 shows the results.

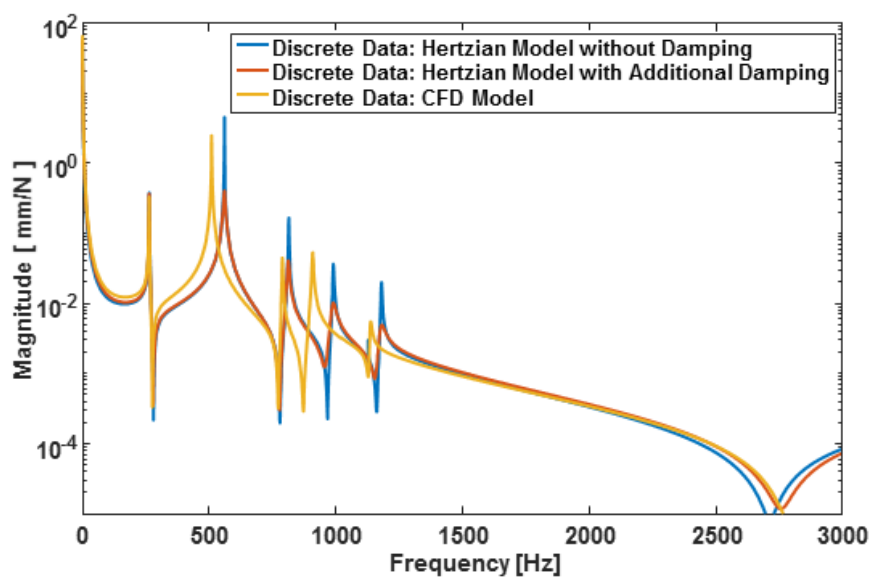


Figure 4.4. LSA results of Testrig w.r.t. excitation: E1 and sensor: S1

Figure 4.4 indicates the difference between three types of models. According to the simulation results, models have the same mode shapes. While the position of resonances are the same position for Hertzian based models, the magnitudes are different due to damping effect. Hertzian model with damping has smaller amplitude. CFD based model has smaller eigenvalues due to smaller stiffness parameter. The magnitude of CFD model is smaller with respect to undamped Hertzian model and larger than damped Hertzian model. The reason is damping values of CFD model larger than undamped Hertzian model and smaller than damped Hertzian model. It is obvious that Hertzian based models and EHD based model leads to different transfer paths in the system.

4.1.2. Experiment and Discussion

The details of the experimental modal analysis are explained in Chapter 2.3.3. To investigate the effect of bearing contact modelling approaches on mechanical system dynamics, an experimental study is conducted using a bearing testrig in WZL. The testrig is designed using simulation shaft-bearing-housing model in Chapter 4.1.1 and results of the experiment is compared with simulation results. The details of the experiment and test results are presented in this chapter.

The bearing testrig has a shaft, housing and two bearings. Bearings are selected as N1014. There are two sensors on different locations. A displacement sensor is placed on shaft, and an acceleration sensor is assembled on housing to obtain frequency responses of the system. Shaft is rotated from 1000 rpm to 5000 rpm and the impulse force is applied to shaft via automatic impulse hammer for extracting the mode shapes and frequency responses. The bearing testrig is shown in Figure 4.5.

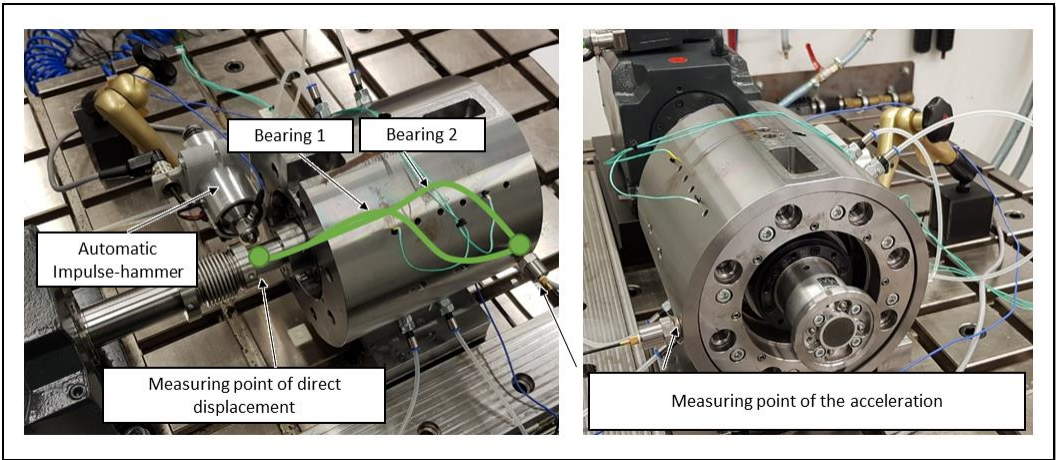


Figure 4.5. Bearing testrig

Figure 4.6 shows the frequency response of simulation and experimental results. According to the results, dynamic behavior of test rig is quite different with respect to simulation results. One of the reason of differences can be operation conditions. Testrig results are obtained, while shaft is rotating. The other reason can be caused from bearing clearance. There is no preload in this setup, and bearing has clearance. Moreover, testrig component stiffnesses also have an impact on test results. It is very difficult, if not possible, to determine the exact values of component stiffnesses and dampings, especially for bushings, bolted contacts etc. All these effects cause non-linearities on system, and the difference between simulation and test results may come from these effects.

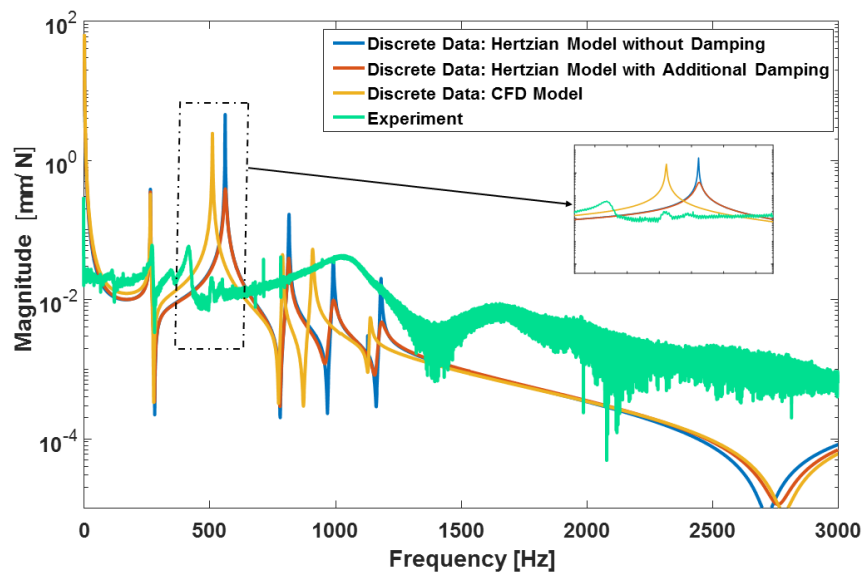


Figure 4.6. Comparison of Simulation and Experimental results

The first peak represents one of the housing modes, shaft and bearing has (almost) no effect on this mode. Therefore, simulation and test results match for this mode. The second peaks show shaft bending mode, and this mode is directly affected by bearing dynamics. According to the zoomed version in Figure 4.6, CFD model has closer results for this mode. Eigenfrequencies show the relation between stiffness and mass properties. Since masses are the same, bearing contact stiffness of CFD model is more realistic than Hertzian model for this mode. However, damping model do not suit well for this mode. As a result, experimental results and simulation results do not match ideally for discrete data models. In order to investigate the bearing contact modelling approaches on system dynamics, continues (subroutine) models are using on eMBS shaft-bearing-housing system in the next section.

4.2. Bearing Simulations Using Continues EHD Characteristic Model

The details of continues EHD characteristic model is explained in Chapter 3. In this part of the study, EHD based (CFD) model is used on eMBS model, and the effect of the bearing model on system is examined. Simpack model 88 Rolling Bearing and Hertzian based bearing contact models are used to compare results. NU308 bearing is selected as bearing type.

The system contains a shaft, two housing parts and two bearings. Bearings have inner and outer rings. While the outer rings are assembled on housing parts, inner rings are located on the shaft. Abaqus software is used to obtain the flexible components of the system. Shaft has two BCs for bearing inner rings and one BC for excitation velocity (or torque) and external applied force. Each Housing part has a BC for bearing outer ring, a BC for fixing the system (to the ground) and a BC for sensor location. BCs are created to form interface between Abaqus and Simpack. Craig-Bampton method is used as model reduction technique and the model are imported in Simpack via FBI file generator. The modelling process is quite similar to the last section model and details are explained in Chapter 4.1. Figure 4.7 shows shaft-bearing-housing model in Simpack.

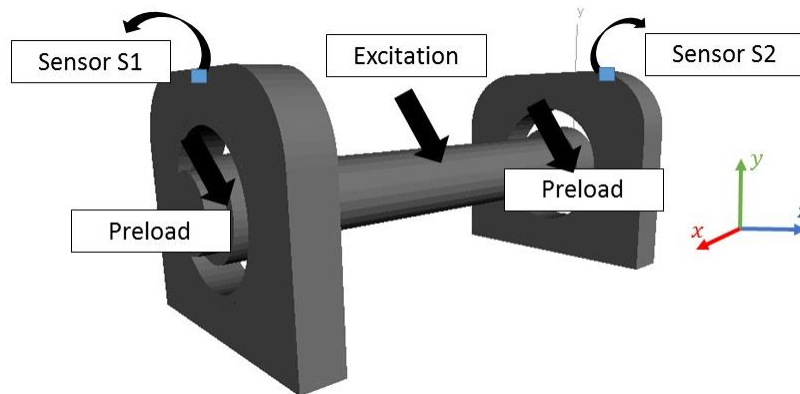


Figure 4.7. eMBS shaft-bearing-housing model in Simpack

The operation conditions are the same of rigid shaft bearing system in Chapter 3.5. The results are obtained both time and frequency domains. The generated force in bearings are examined in time domain, and LSA results are obtained for three different models. The velocity and force dependencies of EHD contact modelling approach is investigated using CFD model in frequency domain.

Figure 4.8 shows the created force in bearings for subroutine Hertzian model, Simpack Model 88 Rolling Bearing and CFD model. According to the Figure 4.8, Hertzian model and CFD model create the same force in radial direction with respect to rolling bearing

model. During simulations, 141.42 N total force acting on a bearing in radial direction due to preloads (100 N in y and 100 N in z directions), and shaft is rotated with 2000 rpm. CFD model is only applicable above 500 rpm, and simulations are conducting using run up velocity profile (0 to 2000 rpm) for CFD model. For under 500 rpm regime, subroutine uses Hertzian calculations, and there is a model switching between 0.8 s and 1 s. The big jump in the middle is due to the model switching between Hertz and EHD models. When the system reaches equilibrium, the generated force in bearings become 141.2 N.

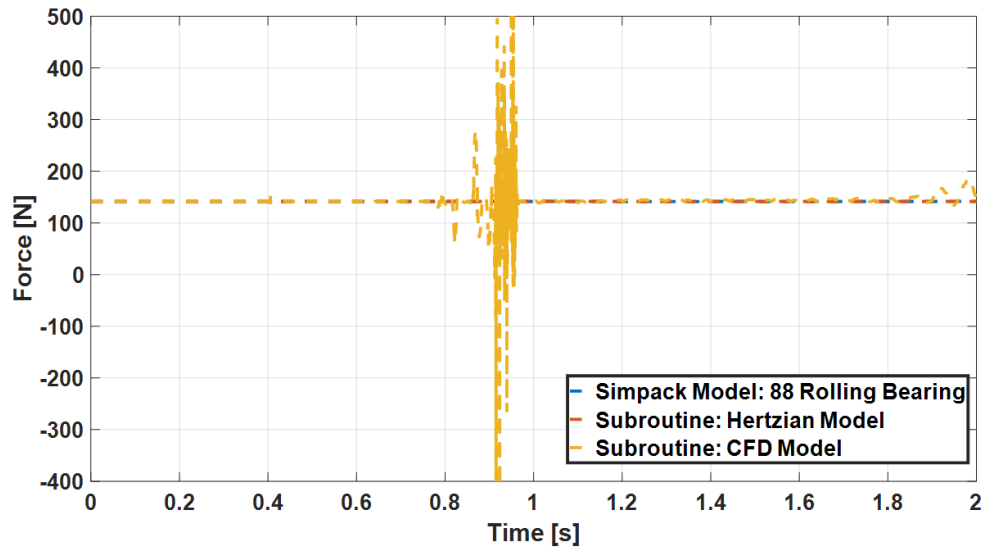


Figure 4.8. Generated total radial force in bearings w.r.t. Excitation: E1, Response: S1
 LSA analyses of the model are presented in Figure 4.9. In simulations a sensor (S1) is located on housing and the acceleration is measured in z direction. Shaft is rotated with 2000 rpm and radial forces acting outer ring to inner ring (141.2 N). The frequency responses of the Hertz and Rolling Bearing models are almost identical for the system. The resonant peaks are related the various shaft bending modes or shaft-housing coupled modes in radial direction. Therefore, the modes are affected by bearing models due to radial movement. Mode shapes of the system (obtained by Simpack Rolling Bearing model) is presented in Figure 4.10. The resonance values have almost the same eigenfrequencies and the magnitudes of the eigenmodes are also quite similar. Results of these two models match ideally.

The mode shapes of the CFD model is identical to the other models. In the literature [2], prestudy and rigid shaft-bearing system simulations, the stiffness values of the CFD modelling approach is smaller than the Hertzian approach, and CFD model includes damping in simulations. As expected CFD model has smaller eigenfrequencies and magnitudes for resonances except frequency 2306 Hz, which is shown in Figure 4.10.

Both CFD and Hertzian based models have almost the same magnitude and location for 2306 Hz mode in Figure 4.10. This mode represents the housing and shaft coupled movement, and housing movement is dominant. The difference may source from these phenomena.

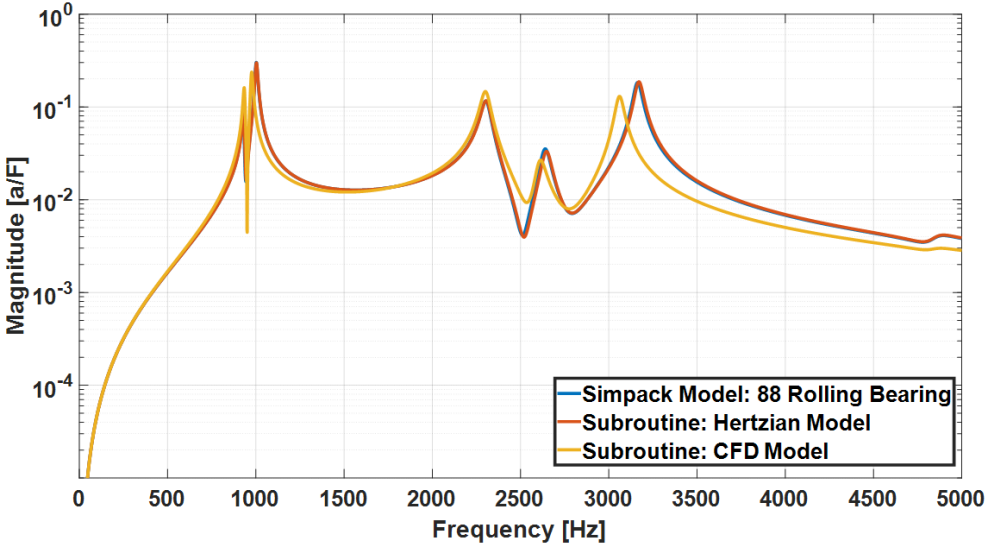


Figure 4.9. LSA comparison of eMBS bearing models w.r.t. Excitation:E1,Response:S1

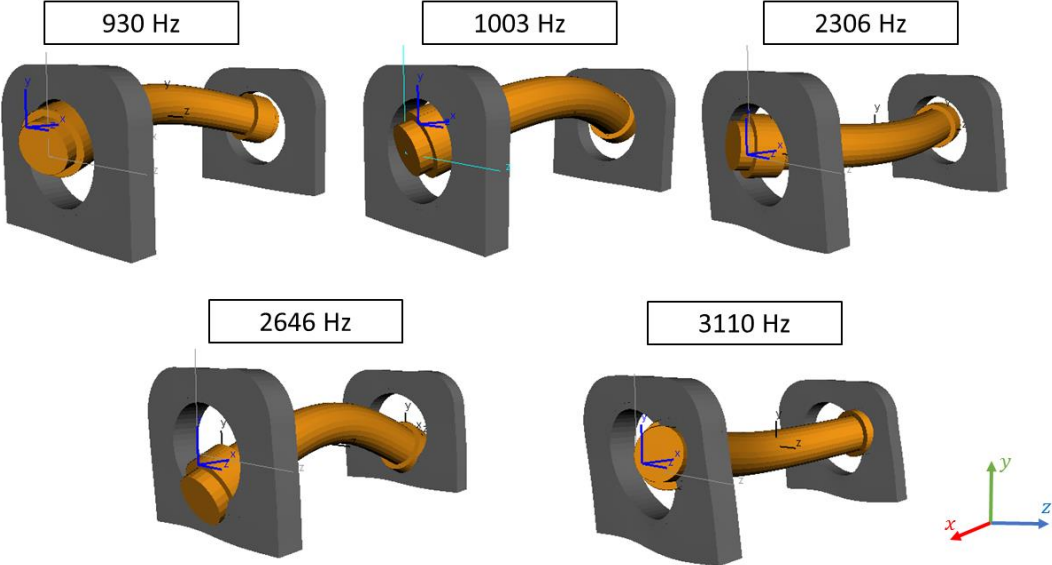


Figure 4.10. Mode Shapes of Hertzian based eMBS models

Figure 4.11 represents LSA results of CFD model for various rotational velocities. According to the results, the resonant peaks of the system show the same eigenmodes on different places. While the angular velocity of shaft is increasing, the resonant peaks should move to the left due to decreasing stiffness and magnitudes should decrease. This situation is clearly observed for the last peak. However, these phenomena is not clearly observed for the other modes. This may due to the sensor location. The sensor measures

the acceleration difference on housing in z direction and only last modes is directly represent the shaft bending mode in z direction.

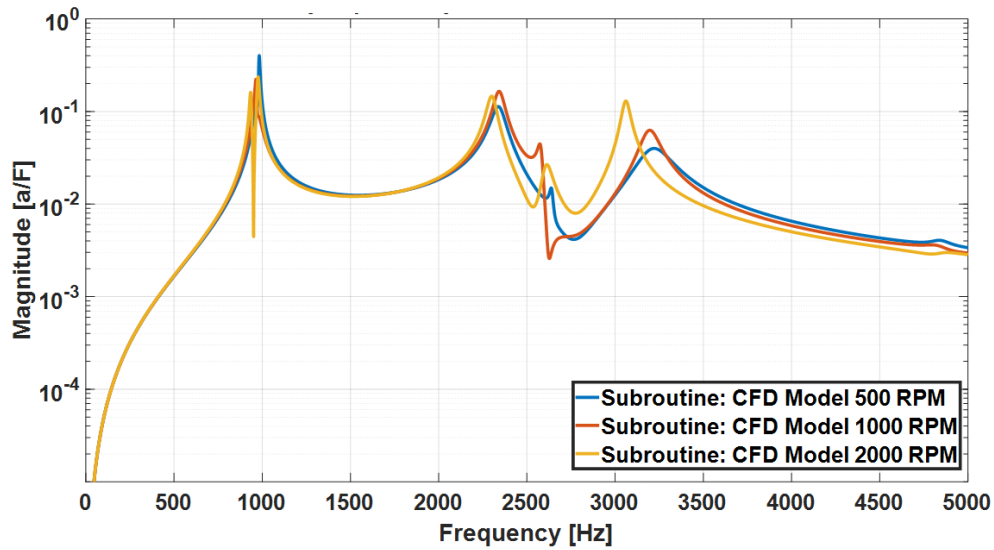


Figure 4.11. CFD model for various rotational velocities w.r.t. Excitation: E1, Response: S1
 LSA results of CFD model for various applied force is shown in Figure 4.12. Simulations are conducted for various radial forces, such as 141.2 N (100 N in y and 100 N in z directions), 212.1 N (150 N in y and 150 N in z directions) and 282.8 N (200 N in y and 200 N in z directions), with 500 rpm shaft rotational velocity. Results are obtained using sensor S1.

According to the results, the last resonance moves to the right due to increasing stiffness, and the magnitudes of the modes are increasing with increasing forces. These result matches with MSE Tribology department report [2]. The other modes do not fit.

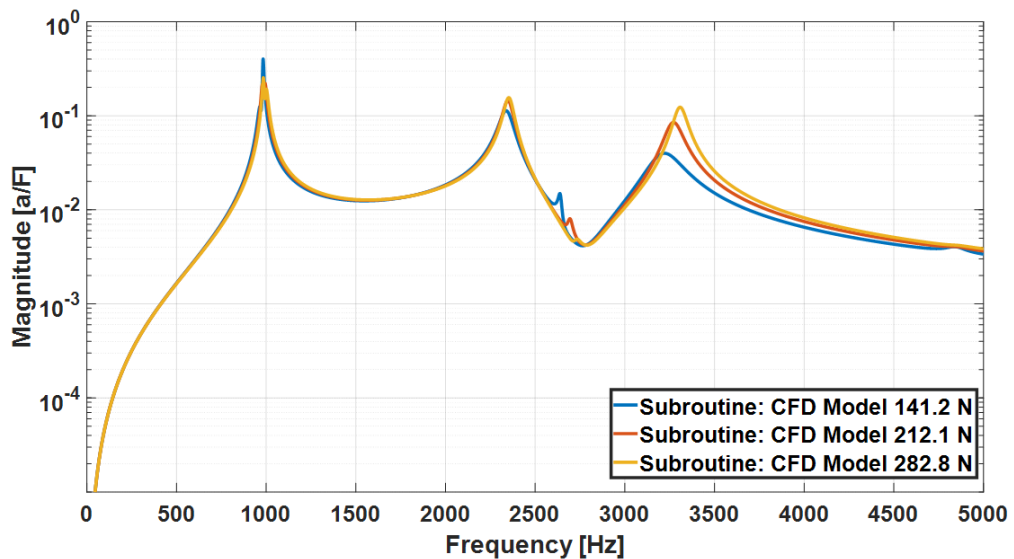


Figure 4.12. CFD model for applied various forces w.r.t. Excitation: E1, Response: S1

5. GEARBOX SYSTEM SIMULATIONS

In Chapter 4, discrete and continuous bearing contact models are used on eMBS shaft-bearing-housing system models. Bearings are main components for radial force generation, therefore shaft-bearing-housing system simulations can be named as bearing level simulations. In order to analyse EHD and Hertzian based bearing contact models detailly, more complex systems should be examined. For this aim, an eMBS gearbox system is built for system level investigations. The flexible system components are created in Abaqus and then transferred into the Simpack via FBI file generator using Craig Bampton model reduction technique. The system has two shafts, a housing part, two gears and four bearings. Shafts are named as input and output shafts, and gears are assembled on shafts. Gears have 21 and 23 teeth, and bearings are selected as NU308. Sensors are located on housing to measure the acceleration. The system in Simpack is shown in Figure 5.1.

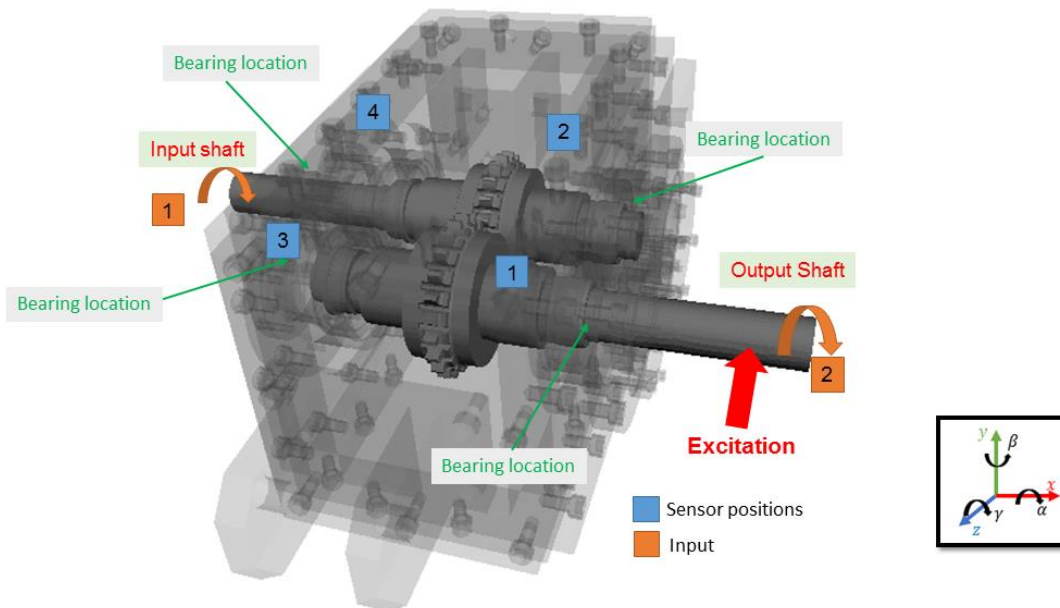


Figure 5.1. Flexible gearbox model in Simpack

Campbell diagram is a 3-Dimensional plot, and it provides information about system dynamic characteristics. The diagram is used to obtain the relation between frequency, velocity and system response. System response is obtained using sensor (output) signal, which can be acceleration, displacement, velocity etc. System resonances are shown in the diagram with their magnitudes, and frequencies. Moreover, the velocity dependencies of resonances are represented as well. Run-up simulations, which have performed with rising velocity profile, are used to obtain Campbell diagram.

In this study, Campbell diagram is used to examine the dynamic characteristics of gearbox model. For this aim, 82 Nm constant torque is applied on input shaft (Excitation E1), and output shaft is rotating with run-up velocity from 500 rpm to 2500 rpm (Excitation E2). Sensor S1 is used to obtain system response as acceleration. Subroutine CFD based bearing model is used to obtain Campbell diagram of gearbox simulation model.

Figure 5.2 shows Campbell diagram of gearbox model with CFD based subroutine. While the linear lines represents gear mesh frequency and its harmonics, vertical lines show resonance frequencies. Linear line colours are changing with magnitudes of response (acceleration). For instance, resonance between 2500 Hz and 3000 Hz has larger magnitude with respect to other resonances and the intersection between the resonance and gear mesh frequency harmonics are red. Resonances in the diagram represents various shaft bending modes, and they are affected by bearing dynamics.

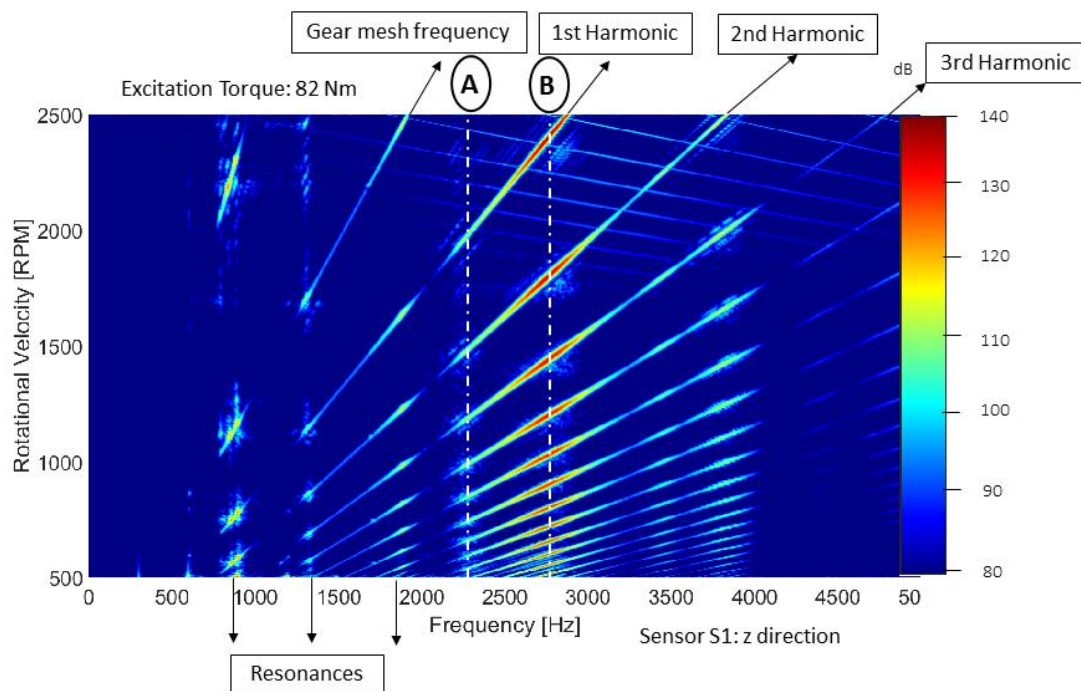


Figure 5.2. Campbell Diagram of eMBS gearbox with subroutine CFD bearing model. The detailed views of Figure 5.2 (section A and B) are shown in Figure 5.3. According to the figure, resonances are affected by operational velocity. White straight lines are added to the diagram, in order to show velocity dependencies of resonances. It is clear that resonances shift to left with increasing velocities, and this situation indicates stiffnesses are decreasing. Black lines are used to create region between 2500 Hz and 3000 Hz. There are harmonics in this region, and the largest magnitudes are observed with respect to other resonances. Between black lines, the high magnitude region is

expanding with increasing velocity. This situation indicates that damping values are decreasing, as operational velocity is increasing.

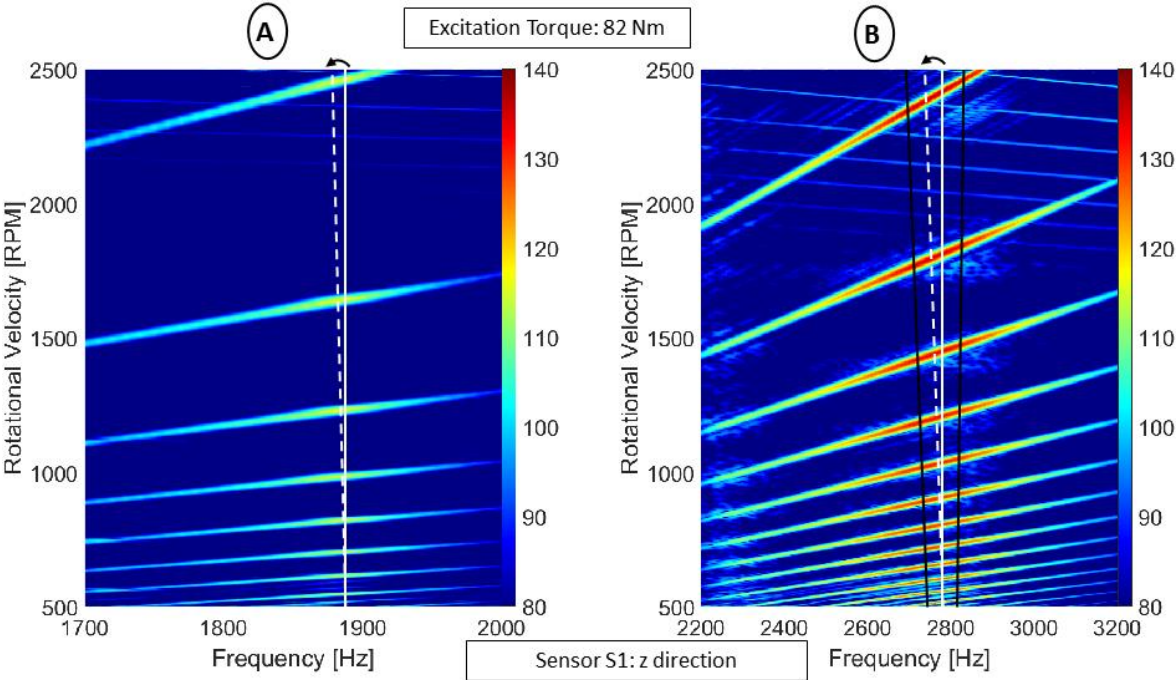


Figure 5.3. Detailed views of Figure 5.2

In order to examine the effect of operational parameters on gearbox system, the transfer path functions in the frequency domain at various velocity states using LSA are calculated and shown in Figure 5.4. Figure shows the velocity dependencies of the system.

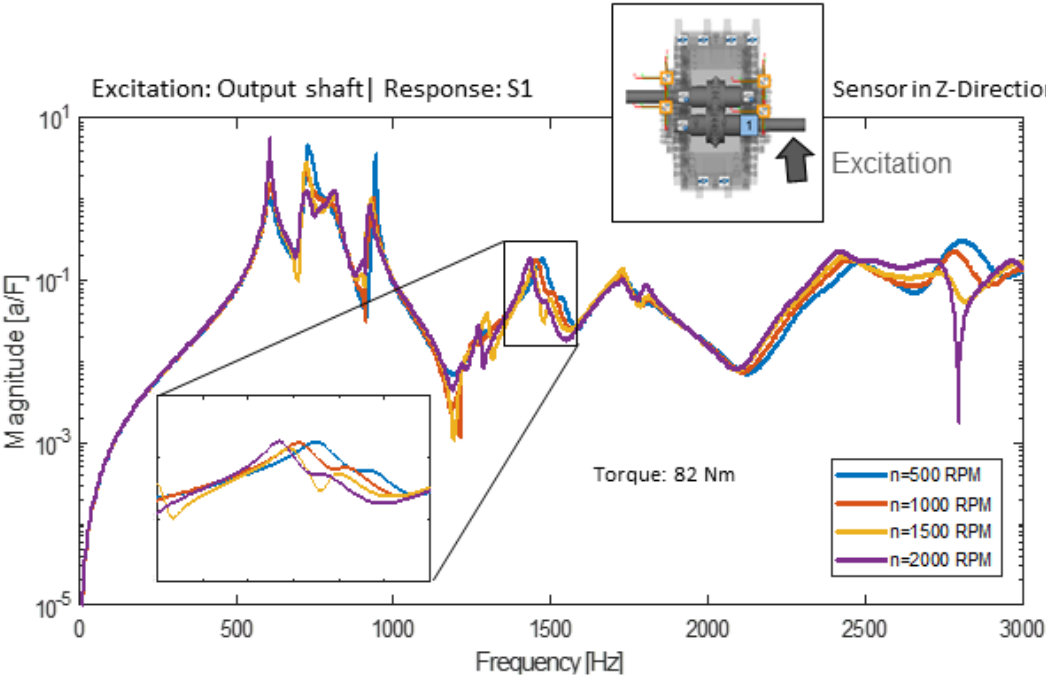


Figure 5.4. LSA results of gearbox

Figure 5.4 indicates that resonances are move to left with increasing velocities. This situation shows that the system stiffness is decreasing with increasing velocity. The amount of shifting is about 3%. Except bearing stiffnesses, other component stiffnesses can be assumed constant in the simulation gearbox model. The gearbox system dynamic behaviour is changing due to bearing dynamics. In order to examine to these phenomena, stiffness and damping parameters inside the bearings are investigated. Figure 5.5 shows changing parameters inside a bearing, which are used in gearbox system.

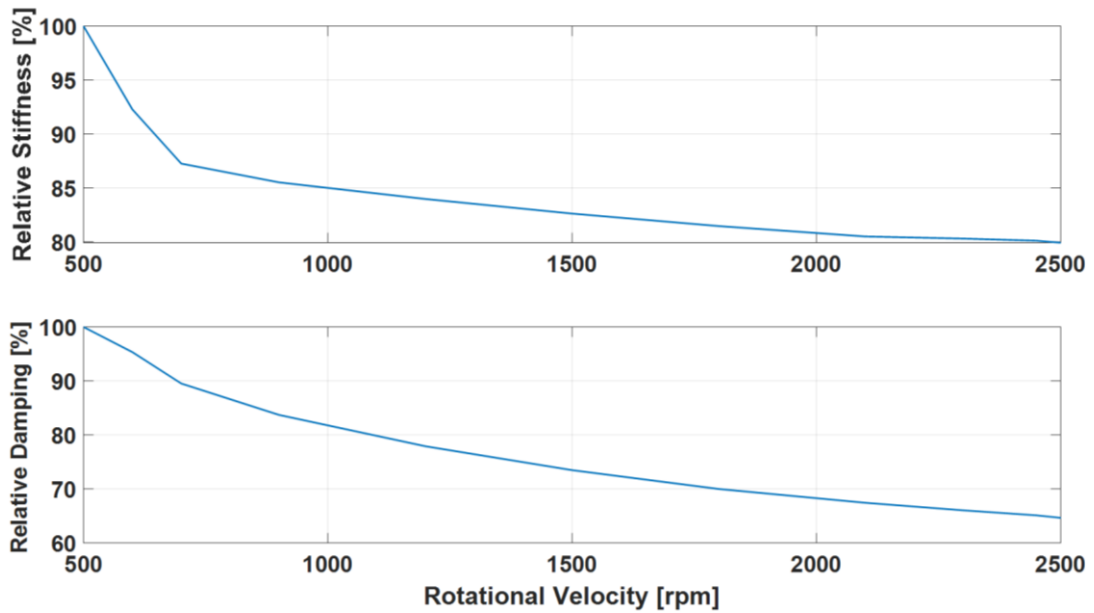


Figure 5.5. Percentage parameter changing in bearing contact

According to the figure, stiffness changing in a bearing is about 20%, and damping changing in a bearing is approximately 35%. The gearbox system model has four bearings and resonance location shifting and magnitude range differences are sources from the bearing dynamic parameters.

Unlike EHD based models, Hertzian based bearing contact models are not affected by operational parameters. The stiffness values of Hertzian based models are determined using geometric and material parameters. For this reason, the dynamic parameters of the model are not changing with rotational velocity. Figure 5.6 shows a Campbell diagram of gearbox, which includes subroutine Hertzian based model without additional damping. Figure 5.2 and Figure 5.6 are obtained using the same operational conditions, and only bearing models are different. White lines show some of the resonances, and the region between black lines indicate damping changing for a resonance. According to the last

figure, there are no shifting for resonances, and no changing for magnitude range. As a result, there are no stiffness and damping shifting.

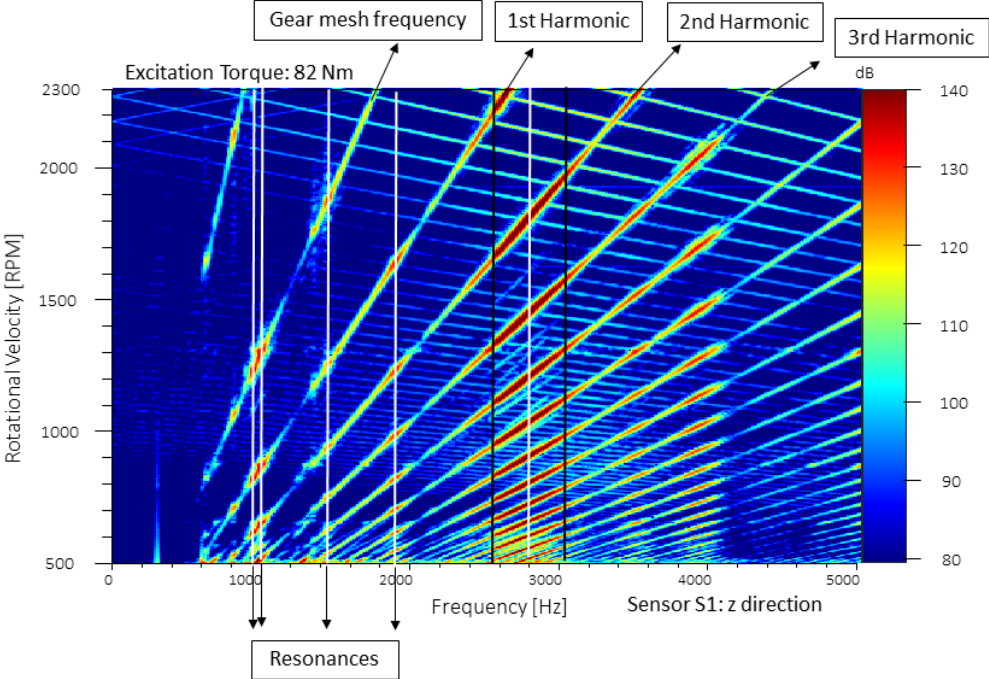


Figure 5.6. Campbell Diagram of eMBS gearbox with subroutine Hertzian based bearing model

6. GEARBOX EXPERIMENTS

In the previous chapters, it was shown that how bearing models are built as subroutines in Simpack, and simulations are performed using these models. In order to investigate the bearing dynamic effects on a mechanical system and validate the simulations in the previous chapter, an experimental study is conducted using a gearbox testrig. The test gearbox is designed the same as simulation gearbox and results of the experiment is used to validate simulation results. The details of the experiment and test results are presented in this chapter.

6.1. Testrig

Figure 6.1 shows a picture of the gearbox used in experiments. The gearbox has an input and output shaft, a housing, two gears and four bearings. Bearings are selected as NU308. Sensors are located on the various positions on housing and acceleration of the housing is measured during experiments. While the excitation torque is applied on input shaft, output shaft is rotated by input shaft with respect to the corresponding gear ratio.

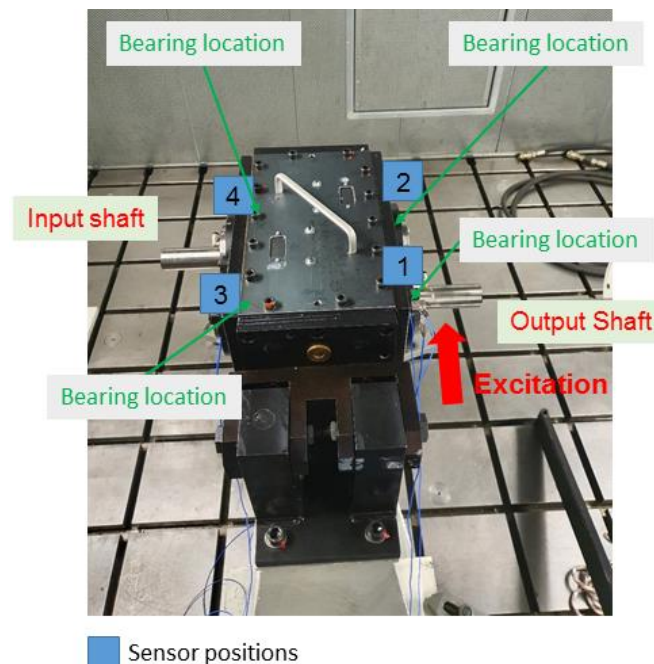


Figure 6.1. Gearbox testrig

There are various operation conditions in the experiment. Torque values are applied from 75 Nm to 305 Nm, and the shafts are reached 2500 rpm as maximum velocities. Different torque and velocity values are used to obtain system frequency responses for various operational conditions. A hammer is used to excite the shaft for extracting the mode

shapes and obtaining frequency responses of the system. The details of the system together with operating conditions are shown in Table 6.1.

Table 6.1. Details of gearbox testrig

Gearbox Datas	
Number of teeth on output gear	23
Number of teeth on input gear	21
Gear Ratio	0.91
Bearing Type	NU308
Oil Type	Shell
Operating Conditions	
Velocity [rpm]	300-2500
Torque [Nm]	75-305

6.2. Results and Discussions

Campbell diagram of gearbox testrig is presented in Figure 6.2. In order to obtain the diagram, 82 Nm torque is applied on input shaft, and output shaft is excited via hammer impulse. Sensor S1 is used to obtain system vibrations. Resonances, gear mesh frequency and its harmonics are shown in the figure.

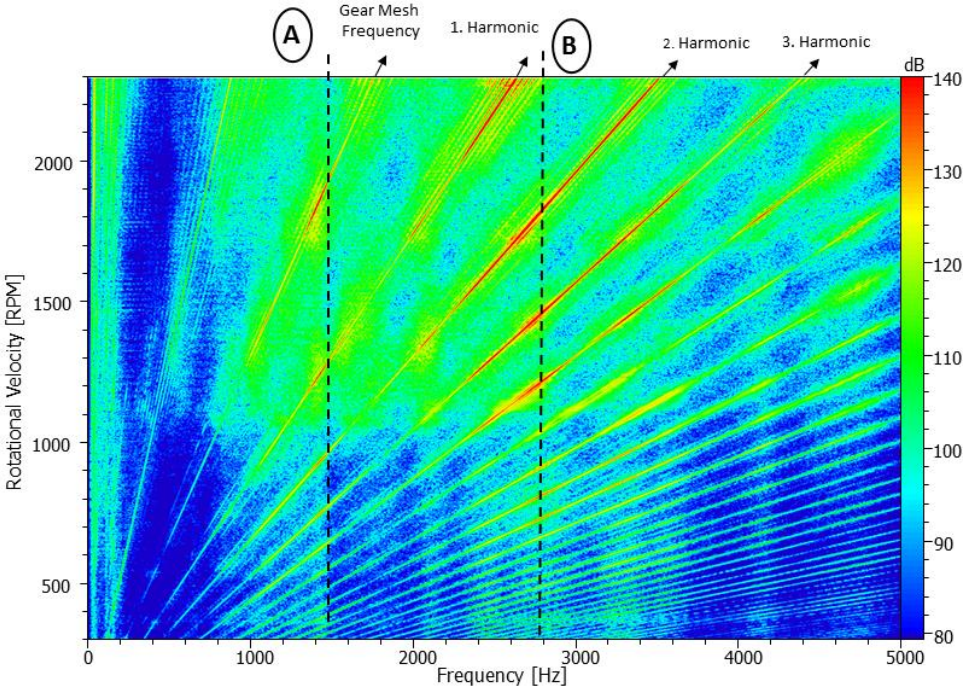


Figure 6.2. Campbell Diagram of gearbox testrig w.r.t. sensor 1

Although various resonances are detected in Figure 6.2, only resonances A and B are analyzed further in details. These resonances are corresponding to the shaft-bearing bending mode. Since bearing stiffness changes due to operational parameters, the system dynamic behaviour is affected by the bearing-shaft bending mode. Therefore, these modes are important to analyze in details. Figure 6.3 shows section A and B. Mode shapes are obtained using simulation model, since testrig gearbox mode shapes match the simulation gearbox mode shapes.

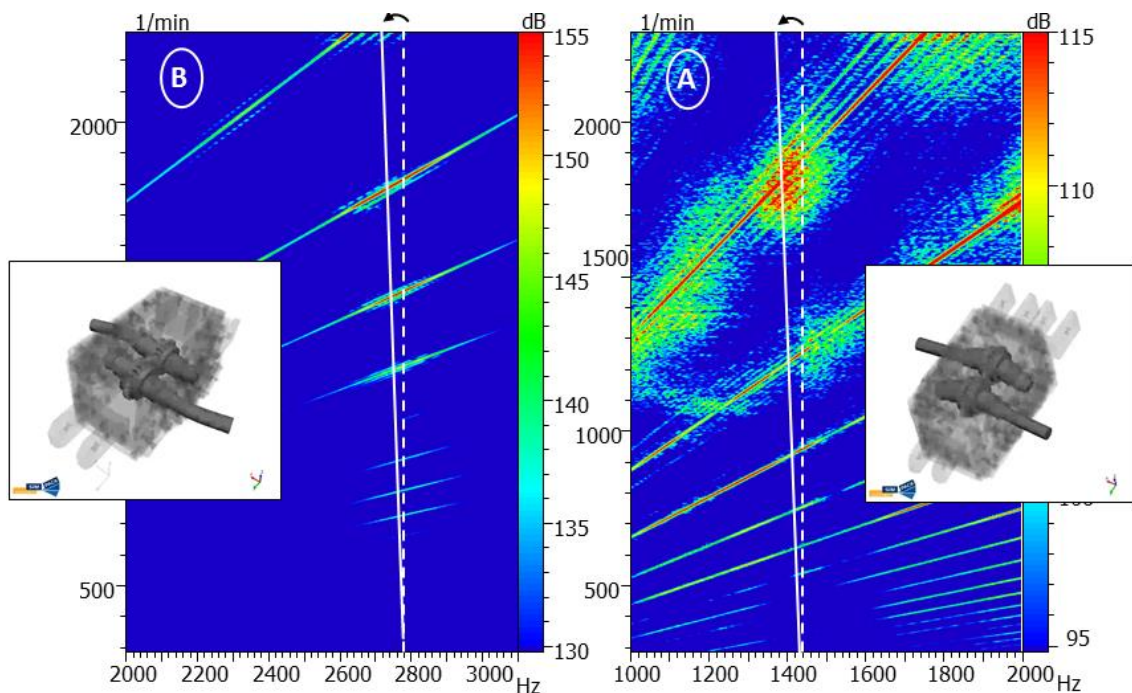


Figure 6.3. Sections from Figure 6.2

According to the figure, system modes move to left with increasing velocity, this means system stiffness is decreasing with rising rotational velocity. These phenomena are also observed for simulation gearbox system with subroutine CFD-based bearing model and not detected for gearbox system using Hertzian-based bearing model. In order to examine the amount of shifting, amplitude spectrums of section A is obtained. Figure 6.4 shows amplitude spectrums of a resonance for two different velocities.

Results in Figure 6.4 indicates a shifting in the resonance to the left by increasing velocity. The amount of shifting is about 3.5%. While shaft rotational speed increases, the thicknesses in the bearing contacts increase. Thus, stiffness of the contact decreases due to amount of fluid in contact increases. This situation can lead to a decrease in the total bearing stiffness, and this means that the bearing-shaft bending natural frequency may decrease.

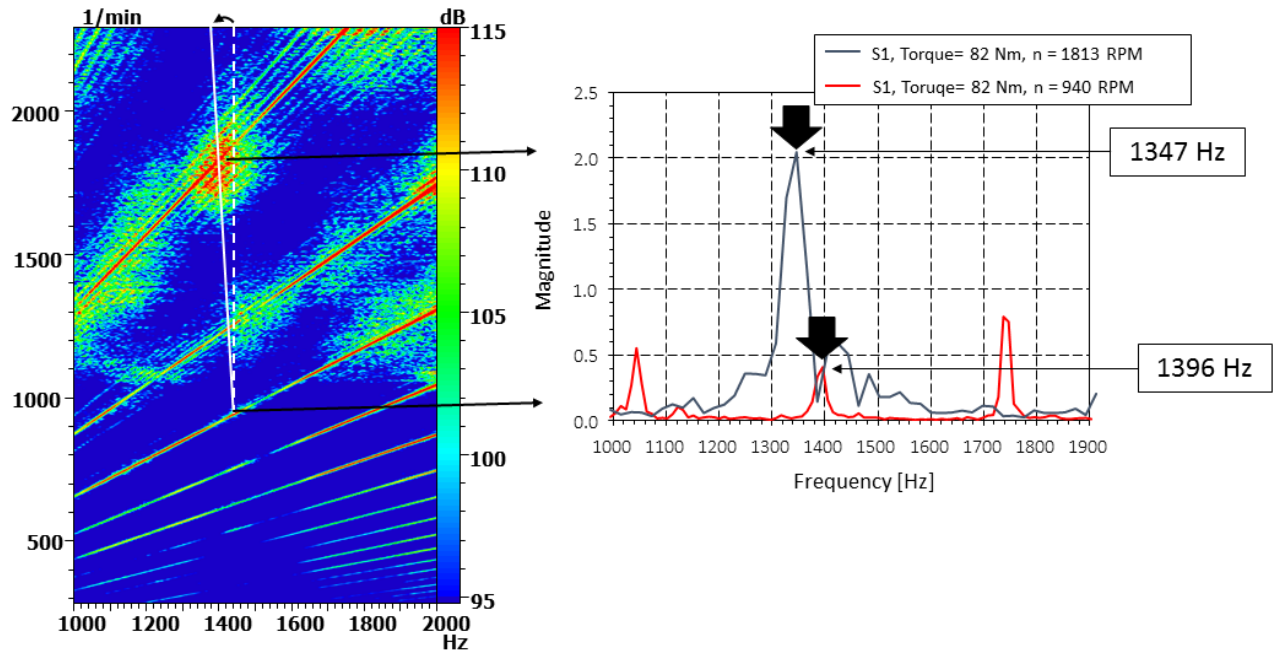


Figure 6.4. LSA results of gearbox testrig for different velocities w.r.t. sensor 1

Another important aspect in dynamic systems simulation which can be considered in the EHD-based bearing model, is the amount and behaviour of the contact damping. In order to investigate the velocity dependency of damping, section B in Figure 6.2 is examined with details. Two simulation model and testrig results are compared each other, and they are presented in Figure 6.5. Figure shows that the resonance area at 2.8 kHz gets wider by increasing velocity in experiment and CFD-based model simulation. As shown in Figure 6.5, the resonance at 2.8 kHz belongs to the shaft-bearing vibration mode in section B. This situation may indicate, damping is decreasing with increasing velocity. This situation can also source from fluid film thicknesses in bearing. As the fluid film thickness increasing, material hysteresis damping is decreasing, hence fluid damping can increase. This causes to decrease in the total bearing damping, which effects to the bearing-shaft bending modes magnitude.

Hertzian based model is not affected by operational velocity, and it does not have damping effect. Therefore, there is no changing observed for Hertzian based model in this region.

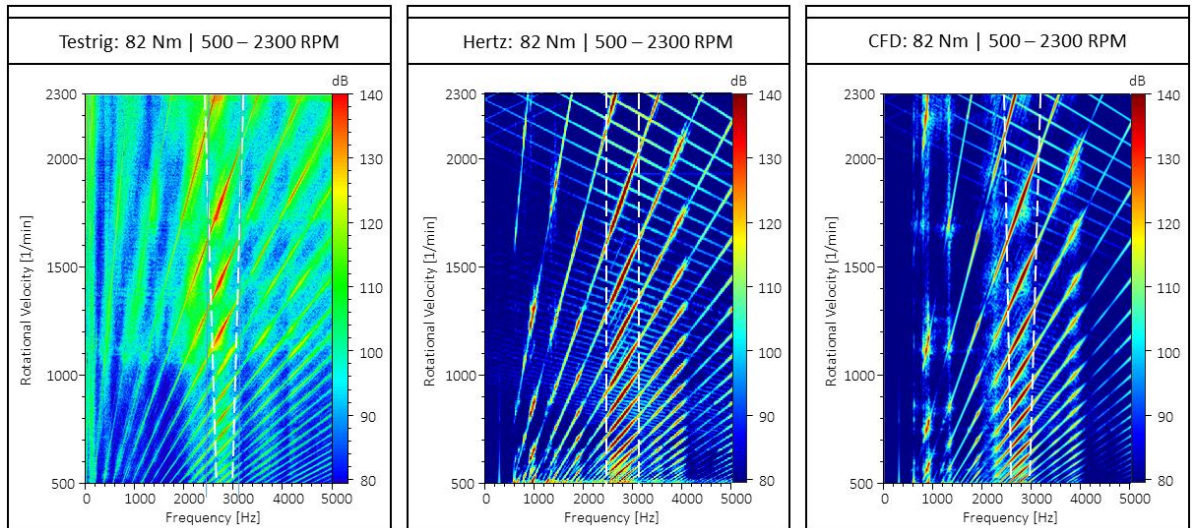


Figure 6.5. Comparison of simulation and test results for section B w.r.t. sensor 1
 In order to validate simulation results, the difference between CFD based model, Hertzian based model and testrig measurements are presented in Figure 6.6, which is obtained using sum level experiment. Overall acceleration signals are used with operational rotational velocity for entire testrig system and the simulation models.

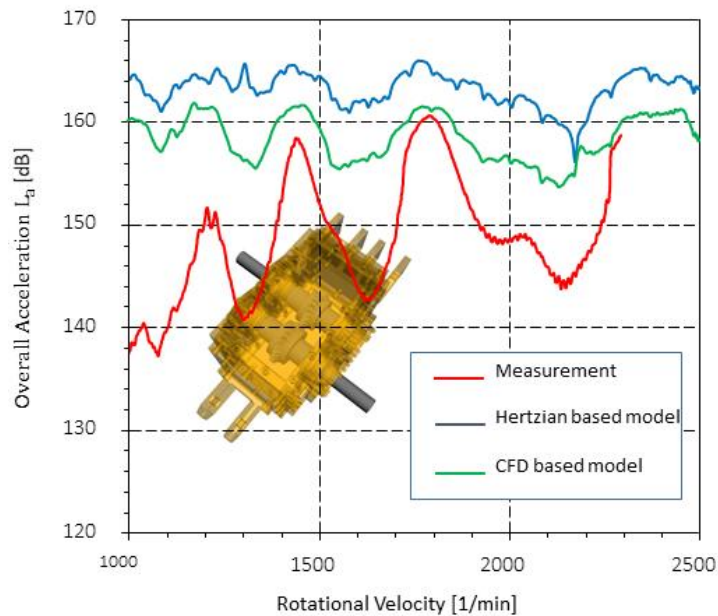


Figure 6.6. Sum level experiment results for various models

Figure 6.6 shows the dynamic behaviour of CFD based model, which matches well with experiment results. The resonance peak locations and magnitudes of CFD based model and measurement results suit, especially after 1200 rpm in the figure. The performance of CFD based model is better than Hertzian based model.

As a result, testrig gearbox measurements show, the dynamic behaviour of the system is affected by velocity. Both stiffness and damping properties are changing with increasing rotational velocity. CFD based simulation model includes velocity dependencies and the results of the model is more realistic and reliable. Hertzian based simulation model does not include velocity dependent parameters. Mode shapes of testrig gearbox and simulation models match, and eigenfrequencies are quite close. For this reason, simulation results are assumed valid.

7. CONCLUSION

7.1. Summary

Dynamic contact modelling of bearing has an important role in Multibody Simulations. The vibro-acoustic transfer functions of the mechanical systems are affected by bearing modelling approaches. There are various aspects of the bearing contact force calculations in literature. While, Hertzian contact calculations are used for solid contacts, EHD approaches are applicable for lubricated contact forces. In order to examine the variations of these models, the force and velocity dependent contact force models are developed. Reynolds and CFD approaches are used to obtain discrete data EHD models, and CFD approach is used to build continuous EHD model. In this study, EHD and Hertzian based contact force calculation models are examined using Simpack.

MBS provides chance to investigate dynamic behaviours of mechanical systems. As MBS mainly focuses on rigid bodies, flexible MBS uses to analyse structural behaviour of the systems. Both rigid and flexible MBS models are built in Simpack, and the frequency response of the developed bearing contact force models are investigated. Shaft-bearing-housing model is created as bearing level simulations, and a gearbox model is created as system level simulations.

Two different validation method is used in this study. Simpack has its own rolling bearing model, namely Force Element 88 Rolling Bearing. Rolling Bearing model is used in bearing level simulations, and results of the simulations are compared with Hertzian and EHD based model simulation results. Moreover, experimental studies are performed via bearing and gearbox testrig. Obtained simulation and experimental results are compared each other.

According to the results of the study, the modelling method of the bearing contact model has a crucial effect on mechanical system vibration transfer path. Hertzian based modelling approach do not consider dependency of operational velocity, and it does not include lubricant damping effect. Unlike Hertzian based models, EHD based models include lubricant damping effect and take into consider velocity dependent stiffness and damping parameters. EHD based model provide relatively 4% less stiffness, and 32% more damping for shaft-bearing-housing system simulation model. The system stiffness is decreasing 4% and damping is decreasing 50% due to increasing rotational velocity for

EHD based model. While stiffness of a bearing is changing about 20% in gearbox model, this effect about 3% system total stiffness.

The results of Simpack Model 88 Rolling Bearing matches well with both CFD and Hertzian based model. Since Rolling Bearing model uses Hertzian based contact calculation method, the simulation results of Rolling Bearing and Hertzian based subroutine model is almost the same. CFD based model simulation results has smaller stiffnesses and eigenfrequencies with respect to Rolling Bearing model simulations due to lubricant effect.

Experimental study on gearbox indicates, system resonances are shifting left, and total stiffness is decreasing about relatively 3.5% with increasing velocity. The lubricant damping effect is observed clearly in experimental results. Mode shapes and eigenfrequencies suit both CFD and Hertzian based model simulations. According to the gearbox testrig results, CFD based bearing contact model provides more reliable and realistic results.

8. REFERENCES

- [1] Teutsch R., Kontaktmodelle und Strategien zur Simulation von Wälzlagern und Wälzfürungen, Doctoral thesis, Institute of Machine Elements, Gears and Transmissions, Technical University of Kaiserslautern, Kaiserslautern, 2005
- [2] Forschungsvereinigung Antriebstechnik e.V., Methodenleitfaden zur simulativen und experimentellen Bestimmung von Lagerübertragungsfunktionen bis in den akustisch relevanten Frequenzbereich, RWTH Aachen University Forschungsvorhaben Nr. 818 I, IGF-Nr. 19788 N.
- [3] T. A. Harris, M. N. Kotzalas, *Essential Concepts of Bearing Technology*, 5th ed.: Taylor & Francis Group, 2006.
- [4] J. Brändlein, P. Eschmann, L. Hasbargen, and K. Weigand, , *Ball and Roller Bearings*. England: Wiley, 1999.
- [5] W. Qian, Dynamic Simulation of Cylindrical Roller, Doctoral thesis, RWTH Aachen University, Institute of Machine Element and Machine Design (IME), Aachen, Germany, 2013.
- [6] *Rolling bearings – Dynamic load ratings and rating life (ISO 281)*, DIN ISO 281, 2007.
- [7] H. Hertz, Über die Berührung fester elastischer Körper, *Journal für reine und angewandte Mathematik*, pp. 156–171, 1882.
- [8] G. Lundberg, Elastische Berührung zweier Hälbraume, *Forschung auf dem Gebiete des Ingenieurwesens*, vol. 10, pp. 201–211, 1939.
- [9] H. A. Rothbart, Ed., *Mechanical Design and Systems Handbook*, 2nd ed.: McGraw-Hill, 1985.
- [10] W. C. Young and J. R. Roark, Eds., *Roark's Formulas for Stress and Strain*, 6th ed.: McGraw-Hill Professional, 1989.
- [11] A. Palmgren, Ed., *Grundlagen der Wälzlagertechnik*, 2nd ed.: Franckh'sche Verlagshandlung, W. Keller & Co., 1959.
- [12] K. Kunert, Spannungsverteilung im Halbraum bei elliptischer Flächenpressungsverteilung über einer rechteckigen Druckfläche, *Forschung auf dem Gebiete des Ingenieurwesens*, vol. 27, pp. 165–174, 1961.
- [13] L. Houpert, An Engineering Approach to Hertzian Contact Elasticity—Part I, *ASME J. Tribol.*, vol. 123, pp. 582–588, 2001.
- [14] Teutsch R. and B. Sauer, An Alternative Slicing Technique to Consider Pressure Concentrations in Non-Hertzian Line Contacts, *J. Tribol.* vol. 126, pp. 436–442, 2004.

- [15] P. Dietl, Damping and Stiffness Characteristics of Rolling Element Bearings, Doctoral thesis, Vienna University of Technology, Vienna, Austria, 1997.
- [16] P. Dietl, J. Wensing, and G. C. van Nijen, Rolling bearing damping for dynamic analysis of multi-body systems-experimental and theoretical results, *Proceedings of the IMechE*, vol. 214, no. 1, pp. 33–43, 2000.
- [17] B. J. Hamrock, *Fundamentals of Fluid Film Lubrication*. Columbus, Ohio: NASA Reference Publication, 1991.
- [18] B. J. Hamrock and Ping Pan, Simple Formulas for Performance Parameters Used in Elastohydrodynamically Lubricated Line Contacts, vol. 246, pp. 246–251, 1989.
- [19] W. M. H. Versteeg, Ed., *An Introduction to Computational Fluid Dynamics: The Finite Volume Method*, 2nd ed.: Prentice Hall.
- [20] T. L. H. Walford and B. J. Stone, The Sources of Damping in Rolling Element Bearings under Oscillating Conditions, *Proceedings of the Institution of Mechanical Engineers, Part C: Journal of Mechanical Engineering Science*, vol. 197, no. 4, pp. 225–232, 1983.
- [21] B. Corves, *Multibody Dynamics Course Notes*.
- [22] S. S. Rao, *Mechanical vibrations*, 5th ed. Upper Saddle River N.J.: Prentice Hall, 2011.
- [23] Dassault Systemes Simulia Corp., *Simpack 2020 Documentation*.
- [24] Dessault Systems Sumulia Corp., *Abaqus 2019 Documentation*.
- [25] R. R.O.Y. Craig and M. C. C. Bampton, Coupling of substructures for dynamic analyses, *AIAA Journal*, vol. 6, no. 7, pp. 1313–1319, 1968, doi: 10.2514/3.4741.
- [26] R. Schelenz, J. Berroth, R. Golafshan, M.Sc., *Maschinenakustik und dynamische Ursachen*, Aachen, Germany, 2020.
- [27] F. Fritz, *Modellierung von Wälzlagern als generische Maschinenelemente einer Mehrkörpersimulation*, Doctoral thesis, Karlsruher Institut für Technologie, Karlsruhe, Germany, 2011.
- [28] D. J. Ewins, Ed., *Modal testing: Theory, practice and application*, 2nd ed.: Research Studies Press Ltd., 2000.
- [29] G. Höpfner, *Estimation of the Gear Mesh Stiffness Using Vibration Analysis*, Master Thesis, Institute of Machine Element and Machine Design (IME), RWTH Aachen University, Aachen, Germany, 2018.
- [30] C. E. Shannon, Communication in the Presence of Noise, vol. 37, pp. 10–21, 1949.
- [31] O. Døssing, *Strukturer Prøven: Teil 1: Mechanische Beweglichkeits-Messungen*. Nærum, Denmark: Brüel und Kjær, 1989.

- [32] Forschungsvereinigung Antriebstechnik e.V., Zylinderrollenlagermodull für Simpack: Entwicklung eines Berechnungsmoduls zur Dynamiksimulation und Betriebsanalyse von Zylinderrollenlagern unter Berücksichtigung der Umgebungskonstruktion in Simpack, Forschungsvorhaben Nr. 625 II, Heft 1234, 2017.
- [33] Tedric A. Harris, Michael N. Kotzalas, *Advanced Concepts of Bearing Technology: Rolling Bearing Analysis*, 5th ed.: Taylor & Francis Group, 2006.
- [34] B. Schlecht, *Maschinenelemente 2*: Pearson Studium, 2010.

CURRICULUM VITAE

Name, Surname : Umut TEKTÜRK
Place of Birth : Ankara, TURKEY
Date of Birth : 12/10/1988
Marital Status : Single
Address : Mamak, Ankara, TURKEY
E-mail : umuttekturk@gmail.com
Foreign Language : English, Deutsch

Education

BSc. : Hacettepe University (2015)
MSc. : -
PhD : -

Work Experience

R&D, MAN Türkiye A.S. (2016 - 2018)
Entrepreneur, Cerntech Engineering (2018 – 2019)
R&D Engineer, DETS Dynamics (2019)
Simulation Engineer, RWTH Aachen University (2019-2020)
MBS Engineer, A-ztech Engineering (2020 -)

